



HAL
open science

Encoding of Temporal Signals by the TGF- β Pathway and Implications for Embryonic Patterning

Benoît Sorre, Aryeh Warmflash, Ali H Brivanlou, Eric D Siggia

► **To cite this version:**

Benoît Sorre, Aryeh Warmflash, Ali H Brivanlou, Eric D Siggia. Encoding of Temporal Signals by the TGF- β Pathway and Implications for Embryonic Patterning. *Developmental Cell*, 2014, 30 (3), pp.334-342. 10.1016/j.devcel.2014.05.022 . hal-02409076

HAL Id: hal-02409076

<https://hal.science/hal-02409076>

Submitted on 13 Dec 2019

HAL is a multi-disciplinary open access archive for the deposit and dissemination of scientific research documents, whether they are published or not. The documents may come from teaching and research institutions in France or abroad, or from public or private research centers.

L'archive ouverte pluridisciplinaire **HAL**, est destinée au dépôt et à la diffusion de documents scientifiques de niveau recherche, publiés ou non, émanant des établissements d'enseignement et de recherche français ou étrangers, des laboratoires publics ou privés.

Encoding of temporal signals by the TGF- β pathway and implications for embryonic patterning

Benoit Sorre^{1,2,§}, Aryeh Warmflash^{1,2,§}, Ali H. Brivanlou^{1*} and Eric D. Siggia^{2*}

1: Laboratory of Molecular Vertebrate Embryology, The Rockefeller University, New York, NY 10065, U.S.A.

2: Center for Studies in Physics and Biology, The Rockefeller University, New York, NY10065, U.S.A.

(§) co-first authors

(*) Correspondence should be addressed to:

E.D.S. : siggiae@rockefeller.edu

A.H.B : brvnlou@rockefeller.edu

Summary

Genetics and biochemistry have defined the components and wiring of the signaling pathways that pattern the embryo. Among them, the TGF- β pathway has the potential to behave as a morphogen: *in vitro* experiments have clearly established that it can dictate cell fate in a concentration dependent manner. How morphogens convey positional information in a developing embryo, where signal levels are changing with time, is less understood. Using integrated microfluidic cell culture and time-lapse microscopy, we demonstrate here that the *speed* of ligand presentation has a key and previously unexpected influence on TGF- β signaling outcomes. The response to a TGF- β concentration step is transient and adaptive, slowly increasing the ligand concentration diminishes the response and well-spaced pulses of ligand combine additively resulting in greater pathway output than with constant stimulation. Our results suggest that in an embryonic context, the speed of change of ligand concentration is an instructive signal for patterning.

Introduction

The morphogen model (Wolpert, 2006) posits that during embryonic development, the morphogen level conveys positional information and determines cell fate. This simple picture is complicated by the fact that morphogen levels in a developing tissue are not static (Harvey and Smith, 2009; Kerszberg and Wolpert, 2007; Lee et al., 2001; Schohl and Fagotto, 2002) and the temporal history of stimulation can have an influence comparable to morphogen levels on patterning (Kutejova et al., 2009). The range of possible dynamic signals that could be encountered during development is quite diverse: a monotone increase patterning the vertebrate Dorso-Ventral axis (Schohl and Fagotto, 2002), the fly wing disc (Wartlick et al., 2011) or the neural tube (Balaskas et al., 2012); oscillatory during somitogenesis (Aulehla and Pourquie, 2010); or pulsatile as recently observed in *Xenopus* animal caps (Warmflash et al., 2012). However, because the dynamics of the ligands that initiate these events in a developing embryo are often hard to discern and to manipulate, it is difficult to disentangle the relative contributions of morphogen levels and dynamics of ligand presentation to the downstream response.

Here we examine how the time course of ligand presentation affects the activity of TGF- β signaling in the myoblast progenitor C2C12 cell line, a model for TGF- β regulated signaling and differentiation (De Angelis et al., 1998; Katagiri et al., 1994; Liu et al., 2001). We adapted an automated microfluidic cell culture platform (Gómez-Sjöberg et al., 2007), that allows us to apply complex time courses of stimulation and record individual cell responses in real time with video microscopy, Fig.S1. Cells grew in

the microfluidic chambers at a rate comparable to that observed in regular cell culture dish and growth was unaffected by either imaging or TGF- β 1 stimulation, Fig.S2. This approach allows a direct and quantitative measurement of the relationship between the dynamics of ligand presentation, transcriptional response and the specification of discrete fates.

The transcriptional response to TGF- β signaling is mediated by the complex of a receptor-activated Smad (R-Smad) with the co-regulator Smad4. Ligand binding to TGF- β receptors leads to R-Smad phosphorylation, complex formation with Smad4, and nuclear translocation (Massagué et al., 2005). R-Smad2/3 responds specifically to Activin, Nodals and TGF- β ligands while R-Smad1/5/8 responds to BMPs and GDFs, Fig.1a. Using cells expressing a GFP-Smad4 fusion, we have recently shown that the response to a step increase in TGF- β 1 was transient and adaptive: Even though the R-Smad, Smad2 and Smad3, remained phosphorylated and localized to the nucleus for as long as TGF- β ligand was present in solution, transcription, measured either by RT-PCR of endogenous target genes or synthetic TGF- β reporters, terminated after about 4 hours (Warmflash et al., 2012), Fig1b-h and FigS2n-p. The C2C12 cell lines stably transfected with fluorescently labelled Smads as reporters responded normally to stimulation when compared to un-transfected cells and the temporal profile of GFP-Smad4 nuclear localization tracked transcriptional activity of endogenous target genes under all conditions examined (Warmflash et al., 2012). The fluorescent Smad4 fusion protein is therefore an attractive reporter of pathway activity since it reveals the immediate consequences of receptor activation, and when co-expressed with a nuclear marker, very amenable to quantitative single cell imaging.

However, in order to understand how pathway activity is interpreted at the level of gene expression, the dynamics of Smad transcription factors should be correlated to the downstream transcriptional response. Traditional population assays destroy the sample, assume homogeneity, and could not practically follow the complex stimuli we apply; we wanted instead to be able to measure transcriptional response in real time and with single cell resolution. For that purpose, we fused a synthetic promoter (Dennler et al., 1998) specific to the Smad3 branch of the TGF- β pathway (CAGA₁₂) to the NanoLuc Luciferase (Nluc), an engineered luminescent protein (Hall et al., 2012) that is over 100x brighter than its *Firefly* and *Renilla* variants and therefore allows for detection of luminescence in single cells, Fig.S1. An identical construct with the NanoLuc replaced with GFP yielded fluorescence below background levels in our cells. Luminescence doesn't suffer from auto-fluorescence or excitation backgrounds and it allows for longer exposure times and therefore greater sensitivity. A synthetic reporter eliminates potential transcriptional feedbacks that could modulate a natural promoter. Since the substrate for NLuc was unstable under cell culture conditions, time-lapse imaging required our microfluidic technology to apply fresh substrate each time an image was acquired and wash it off afterwards, minimizing toxicity. Periodic exposure to substrate also conveniently destabilized NLuc, thus lowering background and revealing the transcriptional response with better temporal resolution. The CAGA₁₂-Nluc induced luminescence could readily be observed using a standard microscopy CCD camera with 2 minute exposure time and addition of TGF- β 1 ligand triggered an 8-10 fold increase of the signal, Fig. 1i-l. See methods, S.I. and Fig.S1 for a complete characterization of our CAGA₁₂-Nluc reporter system.

To establish how C2C12 cells encode different levels of morphogen and to make sure cells behaved the same way in the microfluidic chip than in a regular cell culture dish, we first asked how cells respond to a step-increase in TGF- β 1 ligand for various concentrations, Fig.1b-f. These time courses of stimulation provide a dose-response calibration and serve as a reference for the more complex temporal stimulations examined below. Culture medium containing different concentrations of TGF- β 1 ligand was renewed every hour to insure proper control over the ligand concentration. Comparison of the dose-response with prior experiments in regular cell culture conditions rules out significant ligand depletion

at low concentrations in the small microfluidic chambers. Consistent with our previous experiments (Warmflash et al., 2012), GFP-Smad4 only localized transiently to the nucleus following the step despite continuous stimulation, Movie S1. Single-cell analysis showed that for all concentrations, the vast majority of cells responded in a graded manner to the ligand step with a pulse that peaks within one hour, Fig.1g-h, S2. We observed that full GFP-Smad4 adaptation depend on cell density, Fig.S2q. In the following, to insure consistency between experiments, we worked in conditions where adaption was complete (initial density \sim 300 cells/chamber). The transcriptional response measured with our CAGA₁₂-Nluc reporter is also transient, Fig.1k.

We used modeling to show that all the time dependent stimuli assayed by Nluc expression were consistent with a simple phenomenological model. Unlike previous modeling work focusing on the molecular details of the pathway (reviewed in (Zi et al., 2012)), our model defines the response with only two rate parameters, a timescale for adaptation and the \sim 5hr Nluc half-life, Fig.1k. See also the methods and supplementary methods section 6 for a complete description of the fitting procedure. The best fit required TGF- β driven transcription to be adaptive with a peak about one hour after a step in ligand stimulation. This agrees with the observed dynamics of GFP-Smad4 and is a further consistency check. Finally, as with GFP-Smad4, the Nluc dose-response is graded with concentration and follows a simple sigmoid, Fig.1l.

Pulsed stimulation increases pathway throughput

We have previously shown that Smad4 pulses repetitively into the nucleus in blastula and gastrula staged *Xenopus* animal caps (Warmflash et al., 2012). To investigate the consequences of pulsing, we stimulated cells with 1 hour pulses of TGF- β 1 separated by 6 hours, and obtained a transient response for each pulse, Fig.2a, Movie S2. Under the same stimulation protocol, the signal from the CAGA₁₂-Nluc reporter approximately doubles from the first pulse to the second and then saturates at a value representing the balance between its production and decay that was fit with the same model and parameters as for the step stimulation, Fig.2b and mathematical supplement. If the protein was stable, its accumulation would simply count the number of pulses. At the single cell level, there is no correlation in the amplitude of response to successive pulses repeated every 6hr, Fig.S3, and pulses of different heights elicit an autonomous response independent of the previous pulse Fig.2d. When the pulse repeat-rate becomes comparable to the adaptation time, there is a diminished response around an elevated plateau, Figs.2c, S3a-l. The single cell responses are reduced in amplitude but still uncorrelated from pulse to pulse, Fig.S3. For an adaptive system, such as the one described in Fig.1, pulsatile stimulation could be a mechanism for overcoming adaptation to continuous simulation and increasing pathway throughput.

C2C12 differentiation is blocked more effectively by TGF- β pulses than continuous stimulation.

We next addressed the consequences of pulsed ligand delivery for cell fate specification. The C2C12 progenitors can differentiate to myotubes when exposed to differentiation medium (DM) and presentation of TGF- β 1 inhibits this differentiation, Fig.2e. Working in a standard cell culture dish, we compared the ability TGF- β 1 to block cell differentiation when presented either continuously during 15 hours or as 3 one-hour-long pulses separated by 6 hours, spanning the same total time, Fig.2f. We controlled for TGF- β 1 lifetime by using the same TGF- β 1 containing media to create the 3 pulses. After 24 hours, we used immunofluorescence to quantify the fraction of cells expressing myogenin, an early marker of commitment to terminal myotube differentiation (Tapscott, 2005), Figs.2e-k and S3m-t. Again, pulsatile stimulation proved to be more effective at blocking differentiation and 2.5 times fewer cells

expressed myogenin in the pulsatile case (p-value $p < 10^{-5}$ vs step simulation) despite the fact that the total duration of ligand exposure was only 3 hours as compared to 15 in the step stimulation. Thus pulsed stimulation with a period exceeding the adaptation time enhances both total transcriptional activity and the regulation of cell fate, and the effect is nearly proportional to the number of pulses (2.5x from 3 pulses). Pulsed stimulation is a general mechanism to bypass internal feedbacks limiting pathway output. This mechanism could be at work in blastula and gastrula staged *Xenopus* animal caps, where all timescales are shorter (Warmflash et al., 2012).

Pathway activity depends on the speed of concentration increase

Another generic property of adaptive systems is that their response depends not only on the level but also on the rate of stimulation (Tu et al., 2008). Adaptation to a step in stimulus suggests that the system filters out slowly changing ligands concentration irrespective of their absolute level. To probe this aspect of the temporal response of the pathway, we stimulated the cells with a linear ramp in ligand at various rates of increase, Fig.3a-d. We found that when the increase is sufficiently fast compared to the adaptation time, the response was comparable to step stimulation. The maximum in the GFP-Smad4 response curve clearly decreased with decreasing ramp rate, Fig.3a-d. The single cell response became more diffuse in slow ramps in comparison to steps, Fig.S4a, as expected for an adaptive system. Again, the transcriptional response measured with the CAGA₁₂-Nluc is consistent with the observation made with GFP-Smad4, as confirmed by the fits, Fig.3e-h, S4 and supplementary methods section 6. The rate of ligand delivery has a pronounced effect on cellular response to TGF- β stimulation: the response to a given *level* can be all or nothing depending on the *speed* at which the concentration has been increased.

Our observation that the speed of increase of concentration is as relevant as concentration itself has important consequences as to how a cell reading the morphogen through an adaptive pathway can learn its position relative to a source. Consider a morphogen that diffuses from a source and is degraded. Its steady state profile is exponential, Fig.4a, but the speed of morphogen increase also depends on the distance to the source, Fig.4b. We can now contrast how two pathways, a “linear” and an “adaptive” one, will respond to this ligand time course and extract positional information. The linear pathway responds only to ligand *level*, Fig.4c, while the adaptive pathway is sensitive to both *level* and *speed* and its response to a step is transient, Fig.4d. Both pathways will produce a response that depends on the distance to the source, Fig.4e-f, however, the fact that the adaptive response peaks well before the linear one reaches steady state would tend to suggest that the time required for a fate decision is much less for cells using an adaptive pathway. This could well confer a fitness advantage in rapidly developing embryos, Fig.4g-h. To test that idea, we have utilized the pathway responses from Fig.4e-f as the input to a gene regulatory network (GRN) (Saka and Smith, 2007) featuring the minimal set of elements to achieve fate determination: mutual repression between fates and bistability, see Fig.4g and supplementary methods section 7. Factor B is more sensitive to TGF- β and is excluded from the region of highest morphogen by repression from A. The GRN responds rapidly so as to track the pathway response, and the bistability then locks in the maximum signal seen by a cell. We chose the parameters of the GRN for each case so that the adaptive and linear models resulted in identical spatial patterns and then compared the time to achieve those patterns. The result is clear-cut: the final French-flag pattern is reached 3 times faster if an adaptive pathway is used to read the morphogen gradient, Fig4h-i.

The dynamic response of the adaptive pathway also has the advantage that it is insensitive to ligand dynamics: a 10-fold decrease in the ligand decay rate leaves the relative response as a function of distance unchanged for the adaptive pathway while it becomes much flatter for cells using a linear

pathway, Fig.4j. Nothing changes with the adaptive pathway in the extreme case that the morphogen does not decay at all, while the linear pathway conveys no information about position in this condition, Fig.4k, S4ij. We term positional information acquired through an adaptive pathway *speed fating*.

Discussion

The influence of the speed of increase of morphogen concentration on cell response has been generally overlooked. This is mostly because the key experiments (*Green et al., 1992; Gurdon et al., 1999*), including our own (*Wilson et al., 1997*), that established that both the activin/nodal and BMP branches of the TGF- β pathway behave as morphogens, i.e. that different concentrations of ligand could give rise to different fates, were performed by delivering ligand steps or short pulses of variable height to isolated *Xenopus* blastula cells, *in-vitro*. More realistic temporal stimuli were not considered. In particular a ligand step does not discriminate between an adaptive response and one that registers level only.

Static and dynamic positional information are not mutually exclusive, and one biochemical pathway can display either behavior or a blend depending on kinetic parameters. Their relative contribution can drift during evolution while the complex downstream transcriptional gene network that assigns distinct fates to pathway output remains invariant (Balaskas et al., 2012; Saka and Smith, 2007). However the adaptive sensing of position is invariably faster, less contingent on ligand parameters such as decay rate, and inherently more robust to slow changes in protein levels or the environment. Bacterial chemotaxis is a good example of this strategy and a phenotypic model similar to ours was used to fit ramp stimuli (Tu et al., 2008). Exact adaptation is not required for speed fating, merely maximal response proportional to the time rate of change.

In our experiments the ligand directly activated the pathway, while in the embryo signaling results from a complex interaction of activators and inhibitors. Nevertheless measurement of Wnt, TGF- β , and BMP signaling in *Xenopus* (Lee et al.; Schohl and Fagotto) show that activation of the associated transcriptional effectors (β -catenin, Smad2, Smad1) increase in time and do so most rapidly in regions associated with the greatest pathway activity (e.g. ventral for BMP4). What matters for speed fating is the temporal profile of pathway activity, which will obviously integrate contributions of both inhibitors and activators.

Negative feedbacks following stimulation, either intracellular through receptor inactivation or extracellular through secreted inhibitors, are a very common feature of the signal transduction pathways that are used throughout development, and would tend to lead to partial adaptation. So, independently of the exact molecular details that are specific to each system, the possibility that the time derivative of a signal confers positional information has to be considered, and dynamic characterization of signaling pathways in terms of input-output should be included in modern morphogen models.

Figure legends

Figure 1

Pathway response to a ligand step is adaptive and graded

a - Components of the TGF- β signal transduction cascade.

b,c,d - Evolution of GFP-Smad4 (green) intracellular localization after a step stimulation with TGF- β 1. Before stimulation GFP-Smad4 is mostly cytoplasmic (b), GFP-Smad4 is re-localized in the nucleus 1 hour after the start of stimulation (c), and returns to the cytoplasm by t=5 hours (d). Bar: 20 μ m.

e - Average nuclear to cytoplasmic ratio of GFP-Smad4 as a function of time in response to a step increase of TGF- β 1 concentration from 0 to 0.5ng/ml (n ~ 400 cells).

f - Dose response curve for GFP-Smad4. The “Smad4 jump” response is defined as the maximum in the Smad4 curve relative to the pre-stimulus baseline (see Fig. S1d). Each point is the average of the jumps of all the cells present in one chamber (n~400). Data from two different chambers are plotted. The response (I) is well fit by the expression: $I = a \times \left(\frac{L}{K+L}\right) + b$, where L is the ligand concentration, $K = 0.20 \pm 0.08$ ng/ml is the inflection point and a and b are two constants (black line).

g,h Statistical analysis of single cell response for a few TGF- β 1 concentrations. The distribution of single cell response amplitude (“jump”) is single peaked and graded with ligand level, (g). Most cells respond within 1 hour of the step up in ligand irrespective of ligand level, (h).

i,j - Evolution of Nanoluciferase (Nluc) signal in single cells after a step stimulation with TGF- β 1. Around 5 hours after of beginning of stimulation, an 8-10 fold increase of the luminescence signal (blue) is observed. Nluc was fused to a nuclear localization signal (NLS) to simplify image analysis. Bar: 20 μ m.

k - Average transcriptional activity downstream of TGF- β stimulation (n ~ 400), as measured by the luminescence signal of the CAGA₁₂-Nluc reporter, as a function of time in response to a step increase of TGF- β 1 concentration. Dotted line: fit of our adaptive model (see supplementary methods section 6)

l - Dose response of TGF- β induced luminescence signal of the CAGA₁₂-Nluc reporter. The response is defined as the maximum in the average luminescence curve relative to the pre-stimulus baseline, normalized by the response to the highest dose (n~400). The response (I) is well fit by the expression: $I = a \times \left(\frac{L}{K+L}\right) + b$, where L is the ligand concentration, $K = 0.24 \pm 0.1$ ng/ml is the inflection point and a and b are two constants (black line).

See also figure S1 and S2

Figure 2

Pulsed stimulation increases pathway throughput and fate regulation.

a – Evolution of GFP-Smad4 nuclear to cytoplasmic ratio (thick line, left axis) in response to a pulsatile stimulation. Period of stimulation is 7 hours.

b – Comparison of the transcriptional activity downstream of TGF- β stimulation, as measured by the luminescence signal of the CAGA₁₂-Nluc reporter, when the cells are stimulated with a step (black) or pulsed (blue) stimulation. Dotted lines: fit using the same model parameters as in Fig. 1k.

c - Same as in (a) but with a period of stimulation of 3 hours, shows that when the frequency of stimulation is increased, the amplitude of the averaged response to each pulses decreases.

d - Same as in (a) but with pulses of variable amplitude showing no memory in the response.

e - Differentiation program of the myoblastic cell line C2C12. DM: differentiation medium, GM: growth medium

f – Experimental procedure, exposure to DM alone is contrasted with continuous 15hr exposure or 3 one hour pulses of TGF- β 1. The concentration was 0.1ng/ml in all cases.

g, h, i – Immunofluorescence staining of the cultures against myogenin (green channel). (g) Control DM only, (h) DM + TGF- β 1 step and (i) DM + TGF- β 1 pulses. Counterstain: DAPI (blue). Bar 100 μ m.

j – Normalized distribution of single cell intensity of myogenin signal for the 3 conditions color coded as in f. Cells can be separated in two populations: myogenin negative, myogenin positive based on fluorescent intensity. For each condition, $n > 10,000$. Vertical line represents the threshold between the 2 populations.

k – Comparison of the percentage of myogenin positive cells, as defined in (f), for the 3 conditions. The pulses are on average 2.5 times more effective than the step in preventing differentiation ($p < 10^{-5}$). Error bars are given by the s.e.m. from 10 randomly selected fields.

See also Figure S3

Figure 3

Pathway activity depends on rate of change

a-d - Evolution of GFP-Smad4 nuclear to cytoplasmic ratio (thick lines, left axis) in response to increases of the TGF- β 1 concentration (right axis) from 0 to 0.5ng/ml (a nearly saturating dose) at various rate of increase.

e-h – Evolution of the transcriptional activity downstream of TGF- β stimulation, as measured by the luminescence signal of the CAGA₁₂-Nluc reporter in response to increases of the TGF- β 1 concentration from 0 to 0.5ng/ml (a nearly saturating dose) at various rate of increase. Dotted lines: fit using the same model parameters as in Fig. 1k.

Figure 4

Speed Fating: an adaptive signaling pathway can extract positional information without a spatial gradient

a - At $t=0$, a morphogen (in blue) is allowed to diffuse in a tissue from a constant source located in $x=0$ (upper panel). The diffusion constant is D and ligand decays at a rate k . In such conditions, the steady state profile of concentration is an exponential gradient with characteristic length $\lambda = \sqrt{D/k}$ (lower panel). Colored circles represent cells at various distances from the source.

b - The temporal profile of ligand concentration, calculated at various distances from the source (x) and for ligand parameters, D, k , characteristic for embryonic development (Muller et al., 2012), show that both the steady state concentration and the speed at which this steady state is reached depend on the distance to the source. Color code in (a) or (f)

c-d Comparison of a linear pathway (c) and an adaptive pathway (d) responding to a ligand step as in (b);. For the “linear” pathway, the response (y) to ligand input (I) is given by the differential equation $\dot{y} = I - cy$, where c sets the time scale of response. The adaptive pathway is defined by the system $\dot{y} = I - cy - 0.25c^2 \cdot x$; $\dot{x} = y$ (see supplementary methods) where again c sets the response time and x is a feedback. The reaction time of both pathways is defined to be identical ($c = 10h^{-1}$) and both of them have an amplitude of response that is linear with the ligand concentration. As a consequence they would show an identical dose-response curve to ligand presented as a step.

e - Response of the linear pathway (c) to the different ligand profiles presented in (b). The linear pathway can extract positional information, i.e. the observed response varies as a function of the distance from the morphogen source. Color code for distance follows panel (f).

f - Response of the adaptive pathway (d) to the different ligand profiles presented in (b) depends on the distance to the morphogen source. However the differentiation decision, defined by the time of the response maximum in the adaptive case or when the response saturates for the linear pathway, can be faster in the adaptive system.

g - Minimal gene regulatory network for fate decision between two fates (A and B) induced downstream of TGF- β pathway activity. Factor A is activated at lower TGF- β levels than B, as depicted by the thickness of the arrows.

h-i- Establishment of a French flag pattern in function of time for a linear (h) or adaptive (i) pathway. Fate A (blue) and B (white) are induced downstream of TGF- β signaling and A represses B as in the GRN described in (g). Fate C (red) represents the default fate (both A and B are off). When an adaptive pathway is used, the final pattern is reached 3 times faster.

j - Comparison of how the two pathways extract positional information from a spreading gradient of morphogen. The adaptive pathway is more efficient at patterning since its distance-response curve is much sharper. Furthermore, response-distance function of the adaptive system is insensitive to changes in morphogen properties (dotted lines, 10 fold decrease in decay rate) while the linear pathway is.

$k=0$ –In the extreme case of no ligand decay ($k=0$) the steady state concentration profile does not depend on position but the adaptive pathway can still extract position information while the linear pathway fails to do so.

See also Figure S4

Methods

Microfluidic cell culture and imaging

Cell Culture Chips were obtained from the Stanford Foundry, and controlled by custom made Matlab interface adapted from the one kindly provided by the Quake laboratory. Prior to C2C12 cell seeding, chambers were coated with 20 $\mu\text{g}/\text{ml}$ Fibronectin from bovine plasma (Sigma) for at least 2 hours. The day preceding the experiment, ~ 100 cells/chamber were seeded. Cells were fed every hour either with growth medium (GM, DMEM + 10%FBS) alone or with GM containing TGF- β 1 according to the time course of ligand concentration shown in figures, except for the experiment shown in Fig.3a where medium was changed every half hour. Fluorescence imaging of GFP-S4 was performed every 15 minutes. Nluc luminescence was acquired every hour and fresh Nluc substrate was provided before each acquisition. Single cell data was extracted using custom made Matlab image analysis routines.

C2C12 differentiation

At confluence ($t=0$), culture medium was switched from GM to either differentiation medium (DM, DMEM + 2% Horse Serum) only or DM complemented with 0.1ng/ml TGF- β 1. TGF- β 1 was presented either continuously for 15 hours (step) or as 3 one hour long pulses each separated by 6 hours. To control for ligand consumption/degradation, the medium used for the first pulse was saved and used for the subsequent ones. All samples were fixed and stained for myogenin (clone F5D, 1:200, DSHB) at $t=24\text{h}$, following standard immunofluorescence protocols, detailed in supplementary methods.

CAGA₁₂-Nluc single cell imaging

TGF- β responsive elements are appealing candidates for a single cell TGF- β reporter system, but unfortunately they didn't produce enough signal for detection at the single cell level when driving expression of either GFP or Firefly luciferase.

We thus switched to NanoLuc luciferase (Nluc), a small (19.1kDa) engineered luciferase commercially available from Promega (Hall et al., 2012). The enzyme is advertised to be 150 fold brighter than other luciferases. It uses furimazine, a coelenterazine analog as a substrate. Unfortunately furimazine is not stable under conventional cell culture condition (half-life $\sim 1\text{h}$). In order to solve that issue, we took advantage of the Cell culture Chip capabilities: the Nluc substrate was kept in a refrigerated container in an oxygen-free atmosphere to prevent its degradation for days. Before each acquisition, fresh substrate (10 μM in dmem) was flushed over the cells and rinsed once the picture was acquired, thus minimizing

cell exposure to the substrate. We observed that this procedure conveniently destabilized Nluc to about half its half-life (~ 5 hours). Single cell luminescence signal was measured every hour. CAGA₁₂-Nluc luminescence could readily be detected in single cells with 2 minutes exposure times (objective: 10x 0.45 NA; camera: Hamamatsu ORCA R2, maximum gain, binning 4). See supplementary methods section 5 and Fig.S1 for a detailed description of the validation of the CAGA₁₂-Nluc reporter system.

Fitting Nluc transcriptional response

In order to quantify the degree of internal consistency among our two reporters, GFP-Smad4 and CAGA12-Nluc, for various dynamic stimuli, we have designed a model with only three essential parameters (after allowing for a scale factor to define microscope camera units) each of which can be tied fairly tightly to a single experiment: the timescale of adaptation ($2/c$), the EC50 of the dose-response curve to TGF- β stimulation (K_I) and the life time of Nluc (τ). At the core of our signal transduction cascade is an adaptive module. See Fig.S4b for a graphic presentation of the model. A linear model for adaptation had the fewest free parameters and proved adequate for our data:

$$\dot{x} = y \tag{1}$$

$$\dot{y} = -\frac{c^2}{4}x - cy + I \tag{2}$$

Where I is the ligand dependent input and y the output of the adaptive module. The response of this module following an input step at $t = 0$ is

$$y = Ite^{-ct/2}, \tag{3}$$

Which is in good agreement with the single cell GFP-Smad4 data, especially the fact that the timescale for adaptation ($2/c$) is ligand independent (Fig.1h). It is worth noting that this is not the case with other commonly used adaptive circuits such as the incoherent feedforward loop where the adaptation time varies with the inverse input level, i.e., I has units of frequency.

Upstream of the adaptive module is a receptor module. The dependence of both Smad4 and Nluc in response to a ligand step L scales as $L/(K_I + L)$, Fig.1, so it is plausible to simply model the receptor module and its connection to adaptation by

$$I = L/(K_I + L) \tag{4}$$

For the transcriptional output downstream of the adaptive module, we used:

$$\dot{z}_1 = \max(0, y) - z_1/\tau \tag{5}$$

$$\dot{z}_2 = z_1 - z_2/\tau \tag{6}$$

where z_1 can loosely be thought of as message, and z_2 as protein (Nluc). The relaxation time τ need not be the same in the two equations, but since the data requires $\tau \sim 5$ hrs, while the adaptive system has a time scale of ~ 1 hr, the time course of z_2 is largely insensitive to how relaxation time is distributed between the two equations, so we made the rates equal, thereby eliminating a parameter that would be impossible to fit. Fits of the Nluc data are presented in Fig.1k, Fig.2b, Fig.3e-h and Fig.S4. a detailed description of the fitting procedure and hypothesis is given in supplementary methods, section 6.

Model for Dynamic Embryonic Patterning

To reinforce the intuition that adaptive systems can infer position from the rate the ligand changes in time, we consider that argument in a more mathematical fashion. As an idealized model of morphogen spreading in an embryo, we consider a ligand (L) that diffuses into the region $x > 0$ with a diffusion constant (D) from an infinite source in $x = 0$ and is degraded at a rate (k):

$$\partial_t L(x,t) = D\partial_x^2 L(x,t) - kL(x,t), \text{ which gives:} \quad (7)$$

$$L(x,t) = \frac{x}{2\sqrt{\pi D}} \int_0^t s^{-\frac{3}{2}} e^{-ks - \frac{x^2}{4Ds}} ds \quad (8)$$

For $t = \infty$, Eq.8 becomes $L(x) = e^{-\sqrt{k/D}x}$, the exponential gradient of morphogen. We have plotted in Fig.4b the temporal profile of ligand concentrations experienced by cells at various distances from the source of morphogen.

We then compare how a linear pathway and an adaptive pathway respond to the ligand profiles calculated from eq.8. For the "linear" pathway, the response (y) to ligand input (I) is given by the differential equation:

$$\dot{y} = I - cy \quad (9)$$

where c sets the time scale of response. The adaptive pathway is defined by the system

$$\dot{y} = I - cy - \frac{c^2}{4}x; \dot{x} = y, \quad (10)$$

where again c sets the response time and x is a feedback (note this is the same system than the one we used to fit the Nluc data). The reaction time of both pathways is defined to be identical ($c = 10h^{-1}$) and both of them have an amplitude of response that is linear with the ligand concentration. As a consequence they would show an identical dose-response curve to ligand presented as a step, Fig.4ef.

Finally, to make the point that the transcriptional output from adaptive system can reach its maximal value and thus infer position well before the ligand reaches its asymptotic value, we have modeled a bistable gene regulatory network (GRN) that captures the output ($y(t)$) of the signaling pathway from

equation (9) or (10) and renders it permanent. This is very consistent with standard embryology, where a signal is applied during a window of competency, at the end of which the fate of the targets is specified and no longer requires the signal.

A minimal model requires two proteins, A, B both bistable. They define three territories in order of decreasing signal level: A ON B OFF (blue stripe in Fig.4hi); A OFF B ON (white stripe in Fig.4hi); both OFF (red stripe in Fig.4hi). This GRN is defined by the arrow diagram in fig.4g or by the system of equations:

$$\dot{A} = m(t) + \frac{A^2}{1+A^2} - \nu_A A \quad (11)$$

$$\dot{B} = \left(m(t) + \frac{B^2}{1+B^2} \right) \frac{1}{1+A^2/K_A^2} - \nu_B B; \quad (12)$$

where $m(t)$ is the time dependent input from morphogen signaling pathway upstream of the GRN. It is a quadratic function of $y(t)$ given by eq.9 or eq.10 with parameters chosen to place the asymptotic expression domains of A, B in defined locations. Results presented in Fig.4hi and supplemental movie S3 show how this GRN assigns cell fate as a function of time. A detailed description of the hypothesis behind this model is given in supplementary methods, section 7.

Author contributions

BS, AW, AHB and EDS designed the research. BS, AW and EDS Performed research. BS, AW, AHB and EDS Analyzed data. BS, AW, AHB and EDS wrote the paper.

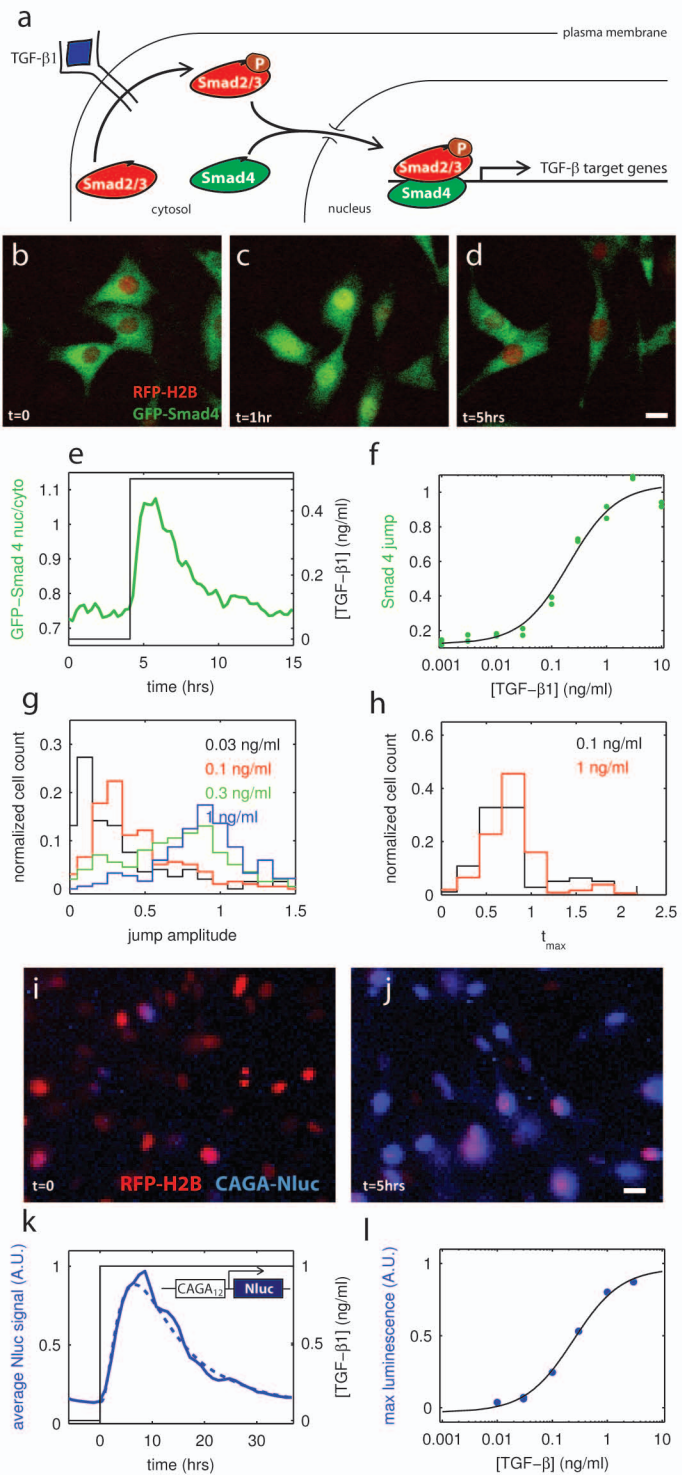
Acknowledgements

The authors are grateful to the members of the Quake and Skotheim laboratories at Stanford University for the help they provided to set up the Cell Culture Chip system in our lab, to Qixiang Zhang and Shu Li for technical assistance and members of the A.H.B. and E.D.S. laboratories for helpful discussions. Funding supporting this work was provided by The Rockefeller University, NYSTEM, National Institutes of Health Grant R01 HD32105 (to A.H.B.) and R01 GM 101653 to (A.H.B. & E.D.S.), National Science Foundation Grant PHY-0954398 (to E.D.S.), the European Molecular Biology Organization ALTF 1476-2010 (to B.S.) and the Human Frontier Science Program LT000851/2011-L (to B.S.)

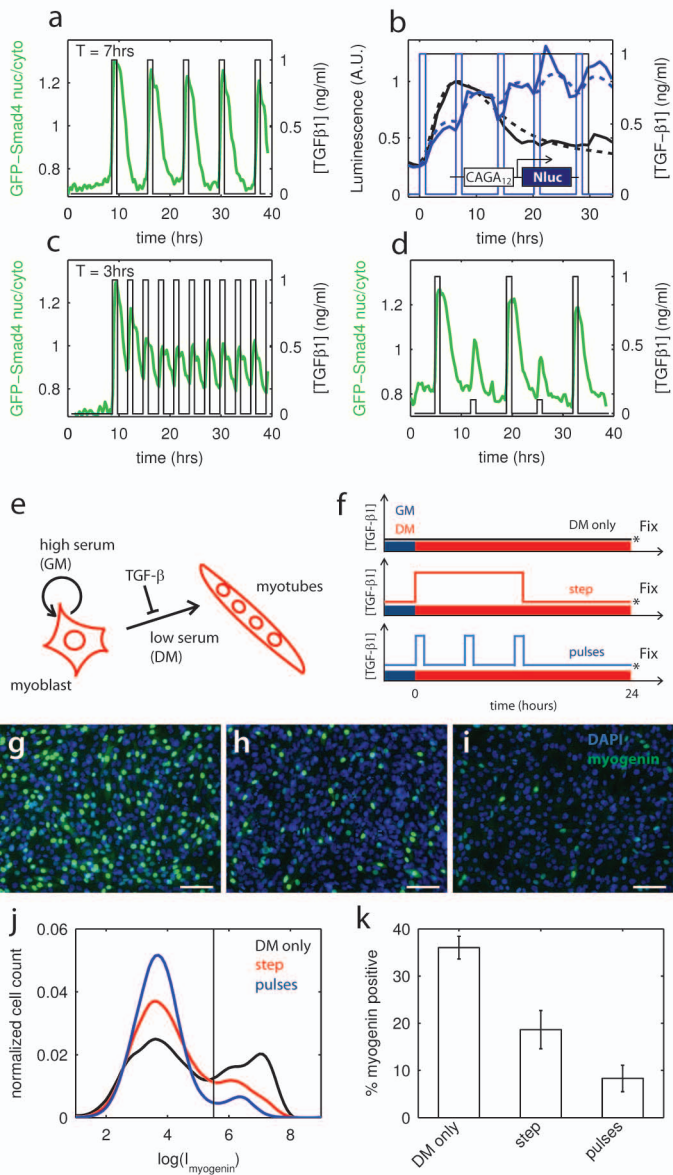
Bibliography

- Aulehla, A., and Pourquie, O. (2010). Signaling Gradients during Paraxial Mesoderm Development. *Cold Spring Harbor Perspectives in Biology* 2, a000869-a000869.
- Balaskas, N., Ribeiro, A., Panovska, J., Dessaud, E., Sasai, N., Page, K.M., Briscoe, J., and Ribes, V. (2012). Gene regulatory logic for reading the Sonic Hedgehog signaling gradient in the vertebrate neural tube. *Cell* 148, 273-284.
- De Angelis, L., Borghi, S., Melchionna, R., Berghella, L., Baccarani-Contri, M., Parise, F., Ferrari, S., and Cossu, G. (1998). Inhibition of myogenesis by transforming growth factor beta is density-dependent and related to the translocation of transcription factor MEF2 to the cytoplasm. *Proc Natl Acad Sci USA* 95, 12358-12363.
- Dennler, S., Itoh, S., Vivien, D., ten Dijke, P., Huet, S., and Gauthier, J.M. (1998). Direct binding of Smad3 and Smad4 to critical TGF beta-inducible elements in the promoter of human plasminogen activator inhibitor-type 1 gene. *EMBO J* 17, 3091-3100.
- Gómez-Sjöberg, R., Leyrat, A.A., Pirone, D.M., Chen, C.S., and Quake, S.R. (2007). Versatile, fully automated, microfluidic cell culture system. *Anal Chem* 79, 8557-8563.
- Green, J.B., New, H.V., and Smith, J.C. (1992). Responses of embryonic *Xenopus* cells to activin and FGF are separated by multiple dose thresholds and correspond to distinct axes of the mesoderm. *Cell* 71, 731-739.
- Gurdon, J., Standley, H., Dyson, S., Butler, K., Langon, T., Ryan, K., Stennard, F., Shimizu, K., and Zorn, A. (1999). Single cells can sense their position in a morphogen gradient. *Development* 126, 5309-5317.
- Hall, M.P., Unch, J., Binkowski, B.F., Valley, M.P., Butler, B.L., Wood, M.G., Otto, P., Zimmerman, K., Vidugiris, G., Machleidt, T., *et al.* (2012). Engineered Luciferase Reporter from a Deep Sea Shrimp Utilizing a Novel Imidazopyrazinone Substrate. *ACS Chemical Biology* 7, 1848-1857.
- Harvey, S.A., and Smith, J.C. (2009). Visualisation and quantification of morphogen gradient formation in the zebrafish. *Plos Biol* 7, e1000101.
- Katagiri, T., Yamaguchi, A., Komaki, M., Abe, E., Takahashi, N., Ikeda, T., Rosen, V., Wozney, J.M., Fujisawa-Sehara, A., and Suda, T. (1994). Bone morphogenetic protein-2 converts the differentiation pathway of C2C12 myoblasts into the osteoblast lineage. *J Cell Biol* 127, 1755-1766.
- Kerszberg, M., and Wolpert, L. (2007). Specifying Positional Information in the Embryo: Looking Beyond Morphogens. *Cell* 130, 205-209.
- Kutejova, E., Briscoe, J., and Kicheva, A. (2009). Temporal dynamics of patterning by morphogen gradients. *Current Opinion in Genetics & Development* 19, 315-322.
- Lee, M.A., Heasman, J., and Whitman, M. (2001). Timing of endogenous activin-like signals and regional specification of the *Xenopus* embryo. *Development* 128, 2939-2952.
- Liu, D., Black, B.L., and Derynck, R. (2001). TGF-beta inhibits muscle differentiation through functional repression of myogenic transcription factors by Smad3. In *Genes & Development*, pp. 2950-2966.
- Massagué, J., Seoane, J., and Wotton, D. (2005). Smad transcription factors. *Genes & Development* 19, 2783-2810.
- Muller, P., Rogers, K.W., Jordan, B.M., Lee, J.S., Robson, D., Ramanathan, S., and Schier, A.F. (2012). Differential diffusivity of Nodal and Lefty underlies a reaction-diffusion patterning system. *Science* 336, 721-724.
- Saka, Y., and Smith, J. (2007). A mechanism for the sharp transition of morphogen gradient interpretation in *Xenopus*. *BMC Developmental Biology* 7, 47.
- Schohl, A., and Fagotto, F. (2002). Beta-catenin, MAPK and Smad signaling during early *Xenopus* development. *Development* 129, 37-52.
- Tapscott, S.J. (2005). The circuitry of a master switch: MyoD and the regulation of skeletal muscle gene transcription. *Development* 132, 2685-2695.

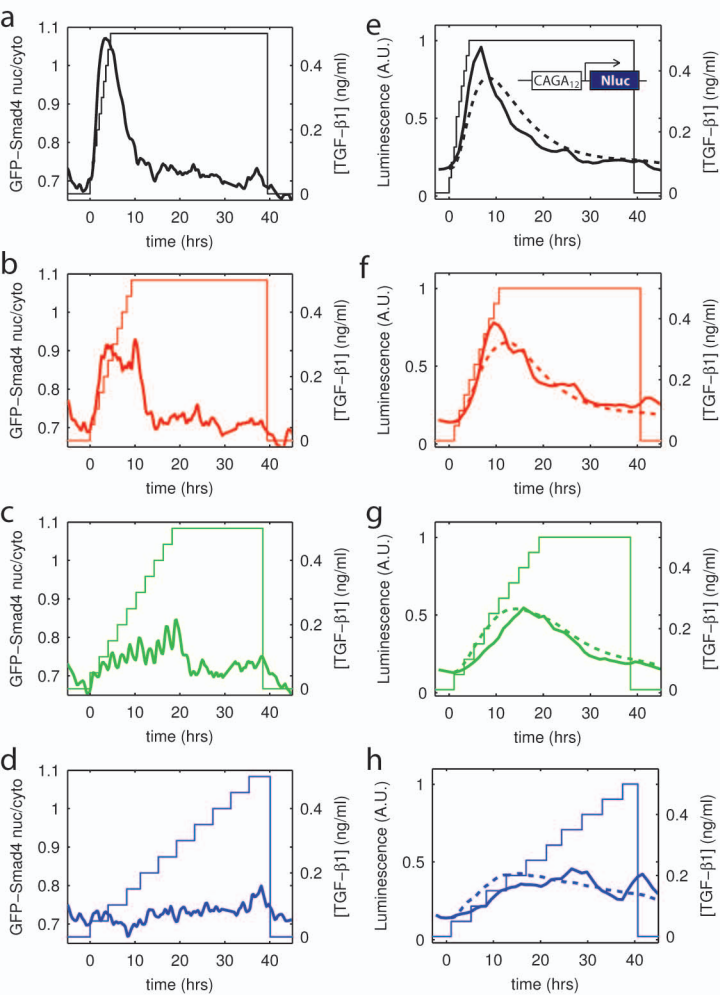
- Tu, Y., Shimizu, T.S., and Berg, H.C. (2008). Modeling the chemotactic response of *Escherichia coli* to time-varying stimuli. *Proc Natl Acad Sci USA* *105*, 14855-14860.
- Warmflash, A., Zhang, Q., Sorre, B., Vonica, A., Siggia, E.D., and Brivanlou, A.H. (2012). Dynamics of TGF- β signaling reveal adaptive and pulsatile behaviors reflected in the nuclear localization of transcription factor Smad4. *Proc Natl Acad Sci USA* *109*, E1947-1956.
- Wartlick, O., Mumcu, P., Kicheva, A., Bittig, T., Seum, C., Jülicher, F., and González-Gaitán, M. (2011). Dynamics of Dpp signaling and proliferation control. *Science* *331*, 1154-1159.
- Wilson, P.A., Lagna, G., Suzuki, A., and Hemmati-Brivanlou, A.H. (1997). Concentration-dependent patterning of the *Xenopus* ectoderm by BMP4 and its signal transducer Smad1. *Development* *124*, 3177-3184.
- Wolpert, L. (2006). *Principles of Development*, 3rd edn (Oxford, UK: Oxford university press).
- Zi, Z., Chapnick, D.A., and Liu, X. (2012). Dynamics of TGF- β /Smad signaling. *FEBS Letters* *586*, 1921-1928.



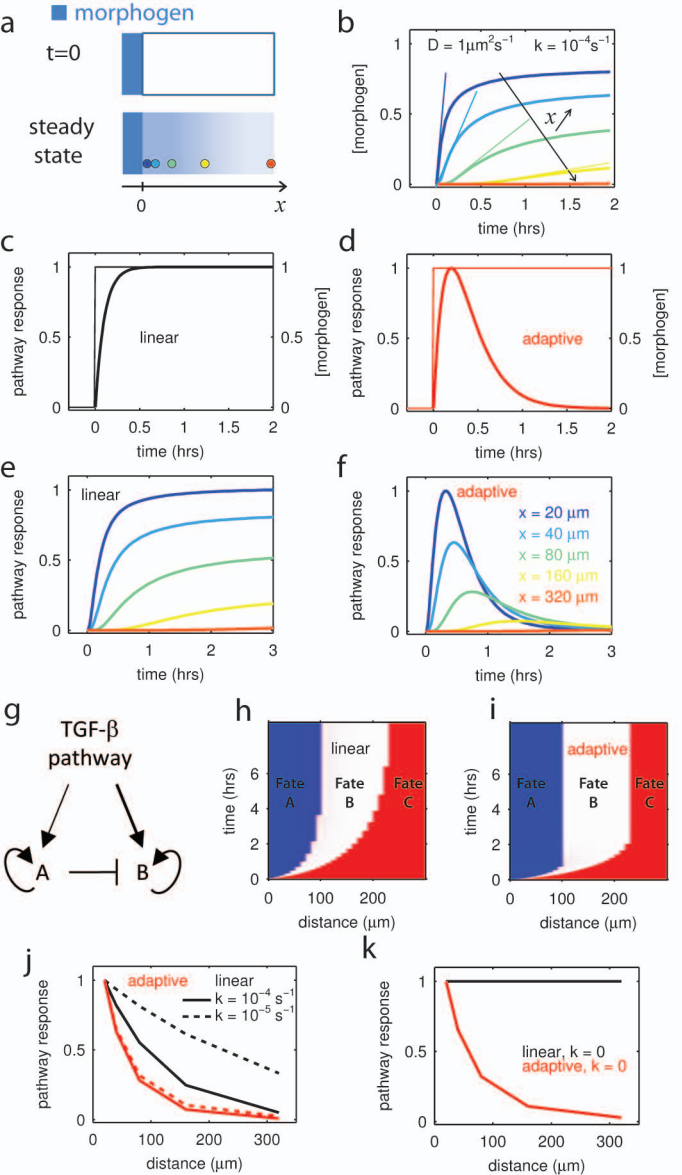
[Sorre et al. Figure 1]



[Sorre et al. Figure 2]



[Sorre et al. Figure 3]



[Sorre et al. Figure 4]

Inventory of Supplementary Materials

Figure S1: Experimental set up. Microfluidic Cell Culture Chip and characterization of CAGA12-Nluc, a live cell reporter for TGF- β pathway transcriptional activity (related to figure 1)

Figure S2: Statistics of step stimulations (related to figure 1)

Figure S3: Effect of frequency of stimulation on the pathway throughput and C2C12 differentiation (related to Figure 2)

Figure S4: Additional figures for mathematical methods (related to figure 4)

Supplementary movie 1 : sorre et al. movieS1 (related to figure 1)

Supplementary movie 2 : sorre et al. movieS2 (related to figure 2)

Supplementary movie 3 : sorre et al. movieS3 (related to figure 4)

Supplementary methods

- 1 - Cell lines, Cell culture, C2C12 cell differentiation
- 2 - Microfluidic cell culture
- 3 - Image analysis
- 4 – Immunofluorescence and Western blots
- 5 - CAGA₁₂-Nluc: a live cell reporter for TGF- β pathway transcriptional activity
- 6 - Mathematical model for fitting Nluc time courses
- 7 - A model for dynamic embryonic patterning

Supplementary references

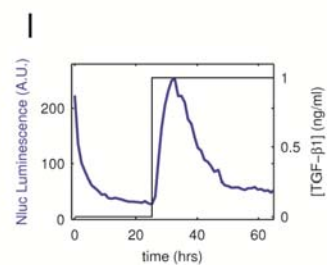
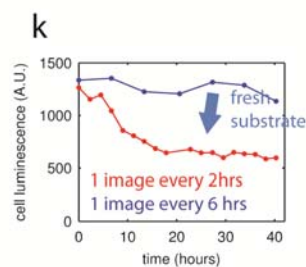
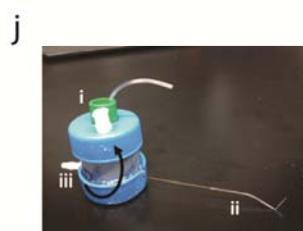
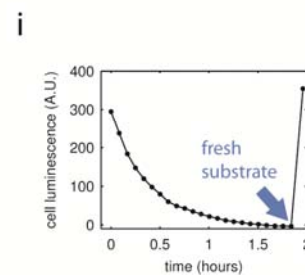
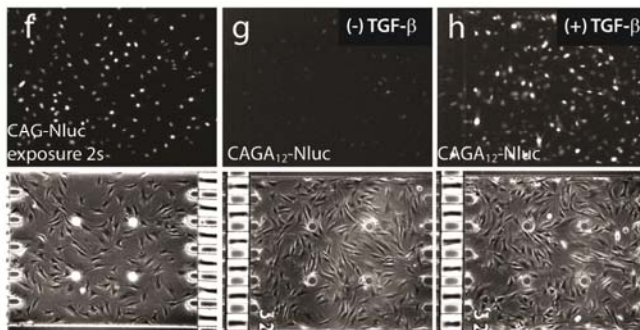
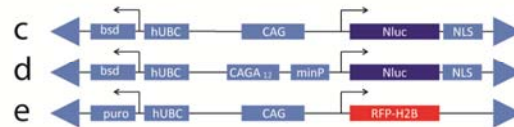
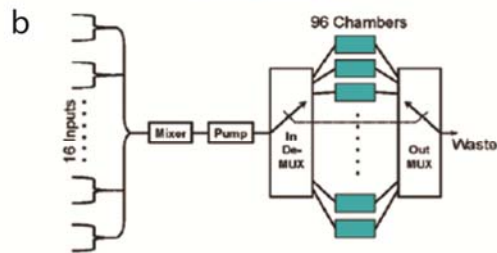
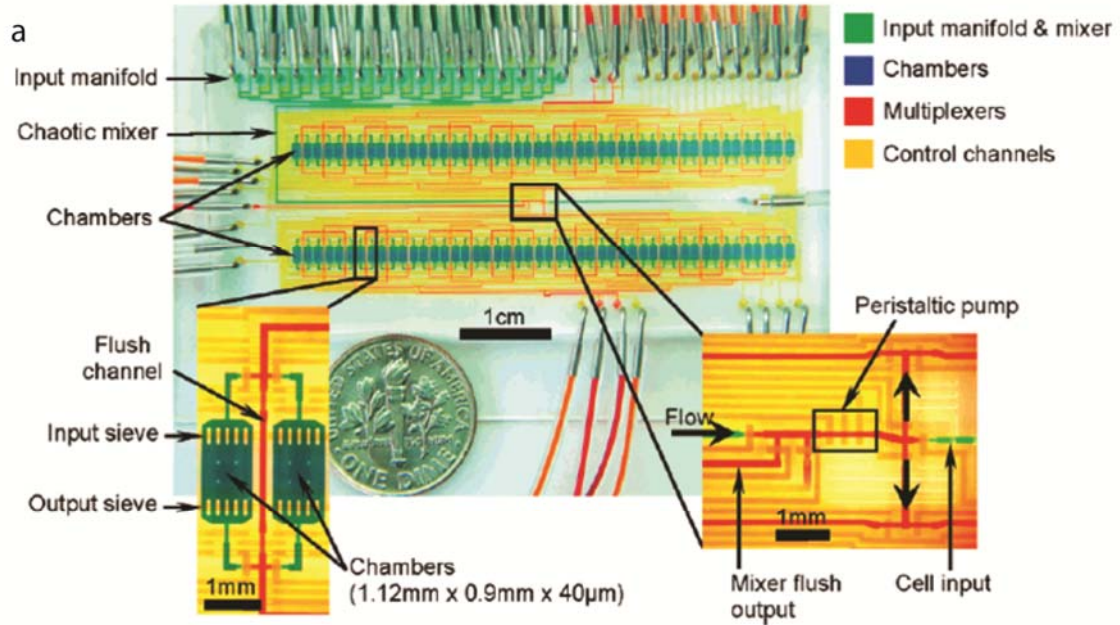


[Figure S1]

Figure S1: Experimental set up. Microfluidic Cell Culture Chip and characterization of CAGA12-Nluc, a live cell reporter for TGF- β pathway transcriptional activity (related to figure 1)

a,b - Design of the cell culture chip. (b) Simplified schematic diagram of the fluidic path in the chip (MUX, multiplexer). (a) Annotated photograph of a chip with the channels filled with colored water to indicate different parts of the device. The left inset gives a closer view of two culture chambers, with the multiplexer flush channel in between them. The right inset shows the root of the input multiplexer, with the peristaltic pump, a waste output for flushing the mixer, and the cell input line. Image and legends for panels a and b were reproduced from ref. ²⁷ (their Fig.1). panels reproduced with authorization of the authors.

(c-e) Constructs used for our NanoLuc luciferase (Nluc), reporter cell lines. (c) To perform controls, a cell line constitutively expressing Nluc under the control of the CAG promoter was engineered. (d) To measure transcriptional response to TGF- β stimulations, we created a clonal line of C2C12 cells with the CAGA₁₂ promoter²⁸ driving Nluc, stably integrated in the genome. C2C12 cells were transfected with ePB-B-CAGA₁₂-Nluc. minP : minimal promoter from pNL3.1 vector, Promega. (e) In both cell lines, we used a constitutive RFP labeled Histone (H2B) to serve as a nuclear marker. Clonal lines were established by plating at single cells densities and selecting clones manually. Nluc was fused to a nuclear localization signal (NLS) to simplify image analysis.

f-h - Top: luminescence picture of a clonal C2C12 cell line expressing NanoLuc luciferase (Nluc) under the control of various promoters. Objective: 10x 0.45 NA; camera: Hamamatsu ORCA R2, maximum gain, binning 4 in the Cell Culture Chip. Bottom: corresponding phase picture. (f) CAG promoter, exposure time 3 sec, (g-h) CAGA₁₂ promoter 2 min exposure time, (g) before TGF- β stimulation and (h) 6 hours after the beginning of TGF- β stimulation

i - Evolution of the luminescence signal measured for the CAG-Nluc-NLS cell line in regular cell culture conditions (35mm, glass bottom dish) at t=0 Nluc substrate is added but the luminescence signal rapidly decays despite the fact that Nluc is constitutively expressed. At t~1.8 hours, luminescence signal is restored by providing freshly reconstituted substrate. This argues that the luciferase substrate is not stable under live cell culture conditions.

j - Homemade refrigerated vial to store NanoLuc luciferase substrate. A cryogenic vial is pressurized from the top (i) with 95%N₂; 5%CO₂ and is connected through the bottom (ii) to the cell culture chip via a fine capillary (ID 75 μ m) to minimize dead volume. The vial itself is enclosed in a small box with one inlet and one outlet (iii) allowing circulation of cold water around the vial. Under typical operation this device keeps the substrate at 10°C in the 37°C live cell incubator.

k - Time course of measured luminescence of C2C12 cells modified to express Nluc-NLS, under the control of the constitutive promoter CAG, in the cell culture chip. Taking advantage of the cell culture chip capabilities, substrate stored in the device presented in (j) is provided just before taking each picture, and rinsed once the picture has been taken. When luminescence was acquired every 6 hours (blue curve) the average signal per cell was constant for up to 40 hours, showing that keeping the substrate cold in an oxygen-free atmosphere successfully prevented its degradation. When the acquisition frequency was increased to one picture every 2 hours (red curve) the measured luminescence initially decays before stabilizing at about half its original value. This suggests that Nluc degrades faster or becomes less effective when it is actively converting substrate to light, and the effective lifetime of nanoluciferase reduced by a factor of 2 under repeated imaging.

I - Full time course of the average luminescence per cell of a clonal C2C12 line expressing CAGA₁₂-Nluc-NLS TGF- β . Luminescence was measured every hour and we waited for it to reach its steady state, typically 15 hours before starting TGF- β stimulation (here a step increase).

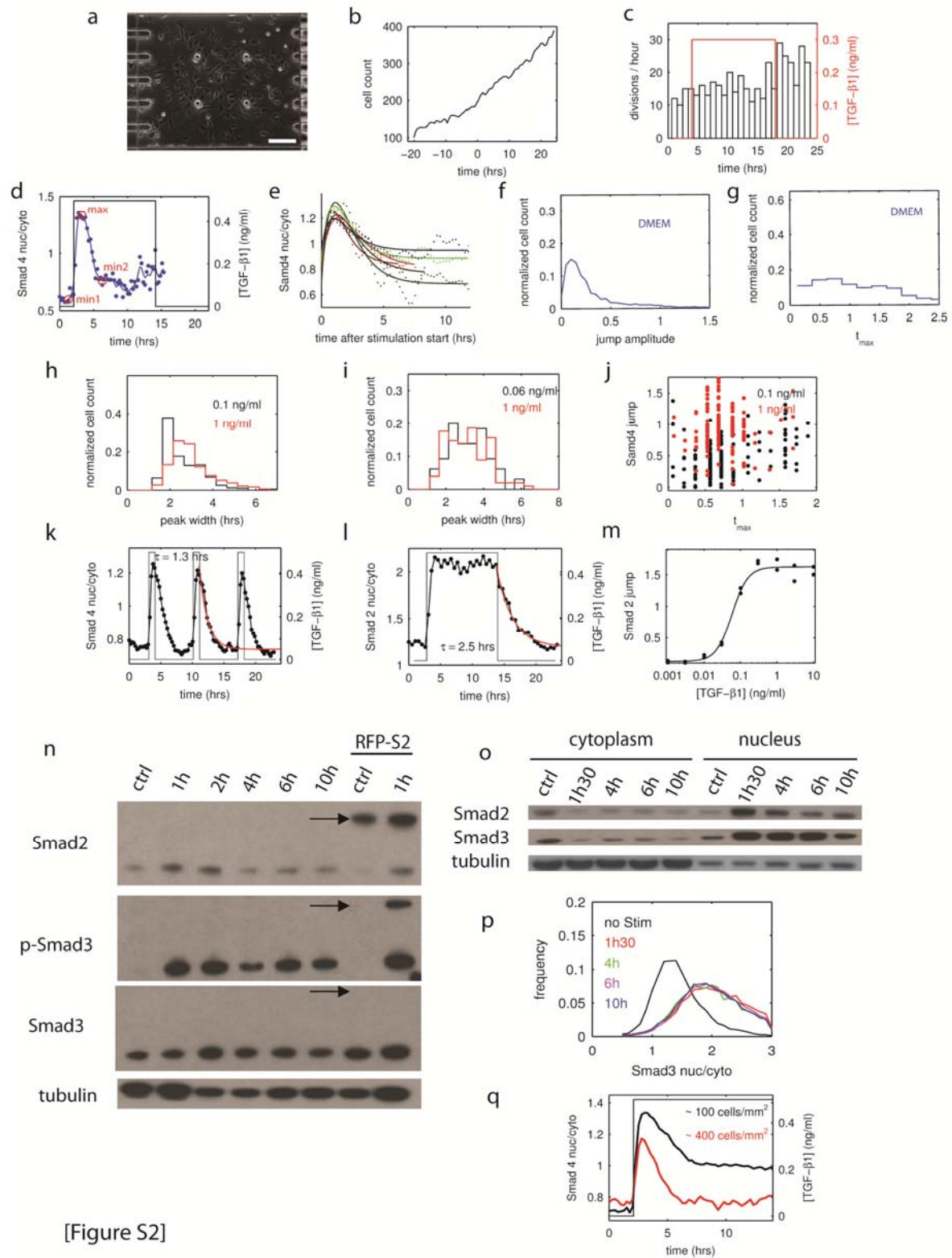


[Figure S2]

Figure S2: Statistics of step stimulations (related to figure 1)

a - Phase contrast image of C2C12 in one of the chambers of the cell culture chip. Note the 4 internal posts that are here to prevent collapse of the chambers. Bar: $200\mu m$.

b - C2C12 cells grow in the cell culture chip at their normal rate (15-20 hours doubling time). Stimulation and fluorescence imaging are started at $t=0$.

c - No change in the birth rate (bar plot, left axis) was observed during stimulation with TGF- β 1 (red line, right axis)

d - Single cell traces analysis. Example of response of one single cell to a step stimulation. For each cell, raw data (blue dots) are spline-smoothed (blue line, matlab curve fitting toolbox) and extrema are computed. We call the cell response the first detected maximum (max) after the initiation of the step, min1 (resp. min2) is the first minimum immediately preceding (resp. following) max. t_{max} , (fig. 1h) is defined as the time at which the Smad4 nuclear to cytoplasmic ratio peaks. The amplitude of the response relative to background, called "jump" (figure 1fg, S2) is defined as: $jump = (y_{max} - y_{min1})/y_{min1}$. A jump of 1 describes a peak value 100% above baseline. The peak width, (fig. S2hi) is defined as: $t_{min2} - t_{min1}$.

e Time scales for adaptation to a step stimulus. Samples of single cell traces after a step stimulation presented in figure 1 e. At $t=0$ TGF- β 1 concentration is increased from 0 to 0.5ng/ml. Single cell traces (dotted lines) are fitted with the expression $y = a \times te^{-t/\tau}$ with $\tau = 1 \pm 0.3$ hours ($n=18$).

f - g background signal of the automated pulse detection. When our pulses detection routine is run on cell traces from an experiment where cell were not stimulated, the routine detects small variation in the single cell traces. However, these detected maxima are not synchronized while even in the case of moderate stimulation, all cells respond within 2 hours after the start of the stimulation (compare with figure 1gh).

h-i Distribution of the temporal width of Smad4 response ($t(\min2)-t(\min1)$ in (d)) to a step stimulation of 2 different TGF- β 1 concentrations shows that peak width is independent of dose. Comparison of cell response in the cell culture chip (h) to the response in a regular cell culture dish (i) shows that in both cases the most of the responses have a temporal width between 2 and 4 hours.

j - Scatter plot of the amplitude of the Smad4 response (jump) as a function of time at which the response reaches its maximum (t_{max}) shows an overall increase of the single cell response for higher dose of TGF- β stimulation, but that the timing of the response is unchanged.

k - l Time scales for decay in the nuclear to cytoplasmic ratio of Smads upon ligand withdrawal. (k) Time scale of decay after ligand withdrawal for GFP-Smad4 nuclear to cytoplasmic ratio. When ligand is removed after 1 hour of stimulation, GFP-Smad4 signal returns to baseline with a time scale of 1.3hrs. The red line is a fit to a regular exponential decay of time scale τ , starting from the time at which ligand is removed. (l) Upon step stimulation, RFP-Smad2 remains nuclear as long as the concentration is maintained and leaves the nucleus with a time scale of 2.5 hrs (red line).

m - Dose response curve for RFP-Smad2. The "Smad2 jump" response is defined as the maximum in the Smad2 curve relative to the pre-stimulus baseline (see fig. S2l). Each point is the average of the jumps of all the cells present in one chamber ($n\sim 200$). Data from two different chambers are plotted. The response (R) is well fit by the expression: $R = a \times \left(\frac{L^2}{K^2 + L^2}\right) + b$, where L is the ligand concentration, $K = 0.06 \pm 0.01$ ng/ml is the inflection point and a and b are two constants.

n – Characterization with western blots of the Smad3 and phospho-Smad3 antibodies on lysates of unstimulated (ctrl) and TGF β 1 stimulated C2C12. To evaluate Smad3 antibodies cross-reactivity with Smad2, we have loaded lysate of a C2C12 cell line expressing Smad2 fused with RFP (higher weight band depicted by an arrow). The RFP-Smad2 is detected by the Smad2 antibody. The Phospho-Smad3 antibody is very specific for the phosphorylated version of the protein, however it partially cross reacts with RFP-Smad2. It is therefore not possible to exclude that the observed sustained response come from Smad2. The Smad3 antibody doesn't cross react with RFP-Smad2. TGF- β 1 concentration in the medium: 1ng/ml.

o – Evolution of the intracellular localization of Smad2 and Smad3 as a function of time after stimulation with TGF- β 1. Smad3, like Smad2 stays localized in the nucleus as long as the cells are stimulated by TGF- β ligand. TGF- β 1 concentration in the medium: 1ng/ml

p –Comparison of histograms of the Smad3 nuclear to cytoplasmic ratio for about 10,000 single C2C12 cells at various times after stimulation. TGF- β 1 concentration in the medium: 1ng/ml

q – Effect of cell density on adaptation to a step stimulation in the cell culture chip. Adaptation is more complete at higher cell densities

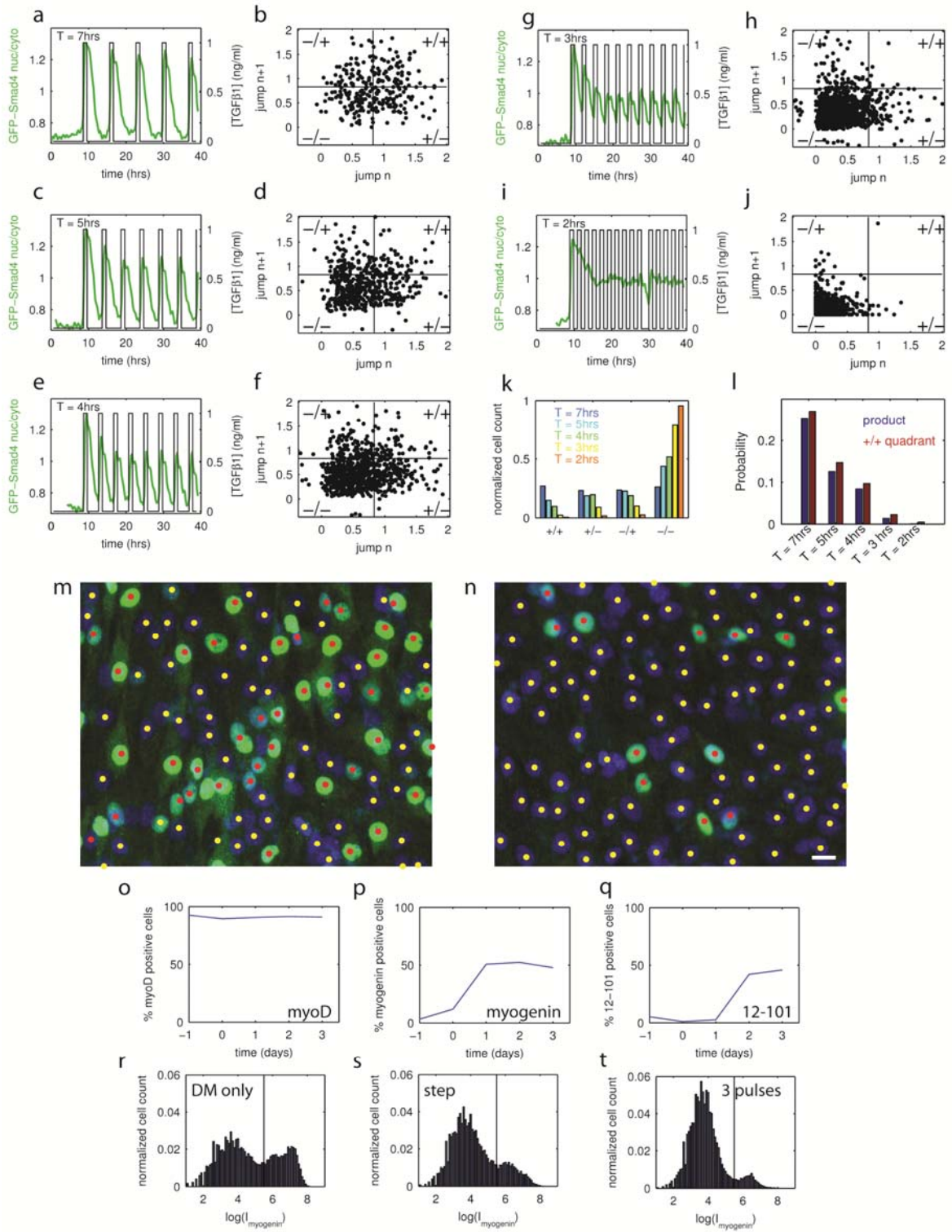


[Figure S3]

Figure S3: Effect of frequency of stimulation on the pathway throughput and C2C12 differentiation (related to Figure 2)

a – Evolution of Smad4 nuclear to cytoplasmic ratio (thick line, left axis) in response to a pulsatile stimulation. Cells are fed every hour either with GM alone or with GM containing TGF- β 1. Time course of ligand is represented by the thin square wave line (right axis). Period of stimulation is 7 hours.

b – The scatter plot of the amplitudes of single cell responses to two consecutive pulses from the experiment presented in (a) shows no correlation between successive pulses for T=7 hours. The center of mass of the cloud of points is used to define 4 quadrants named -/- for two consecutive low responses, -/+ and +/- when a low (high) response is followed by a high (low) response (respectively) and ++ for two consecutive high responses.

c-d Same as in (a-b) period of stimulation 5 hours.

e-f Same as in (a-b) period of stimulation 4 hours.

g-h Same as in (a-b) period of stimulation 3 hours.

i-j Same as in (a-b) period of stimulation 2 hours showing the response merges into a plateau as in Fig. 1e.

k - Evolution of the relative proportions of cell response in the 4 quadrants defined in (b) for 5 frequencies of stimulation, shows that when stimulation frequency is increased, individual cell response decreases progressively.

l - Probability of two high responses following each other (++ quadrant, $P_{+/+}$) is not significantly different from the product of the probability for a high response at the first pulse to the second (product, $(P_{+/-} + P_{+/+}) \times (P_{-/+} + P_{+/+})$), shows that the response to two successive stimuli is uncorrelated.

m-n Automated cell counting and measurement of single cell myogenin signal. Cells are stained for myogenin (green) are counter-stained with dapi (blue). Cells counted as positive (resp. negative) for myogenin are marked by a red (resp. yellow) dot.

m - Cells stained after one day in differentiation medium without TGF- β 1, as in figure 2g.

n - Cells stained after one day in differentiation medium, during which they received 3 one-hour pulses of TGF- β 1, as in figure 2i. Bar 20 μ m.

o-p-q Time course of expression of 3 myogenic markers. At day 0, cells are confluent and medium is switched from growth medium (GM) to differentiation medium (DM). The myoblastic marker myoD stays on during the complete time course of differentiation (o). myogenin, an early marker of commitment to terminal differentiation to myotube is present in about 50% of the cells after one day in differentiation medium but was absent under proliferative conditions. 12-101, a marker of

terminal muscle cells differentiation is detected only after the second day in differentiation conditions.

r-s-t Unsmoothed version of the histograms presented in figure 2j, the vertical bar represents the threshold between myogenin positive and myogenin negative cells. (f) DM only, (g) DM + TGF- β 1 step and (h) DM +3 TGF- β 1 pulses

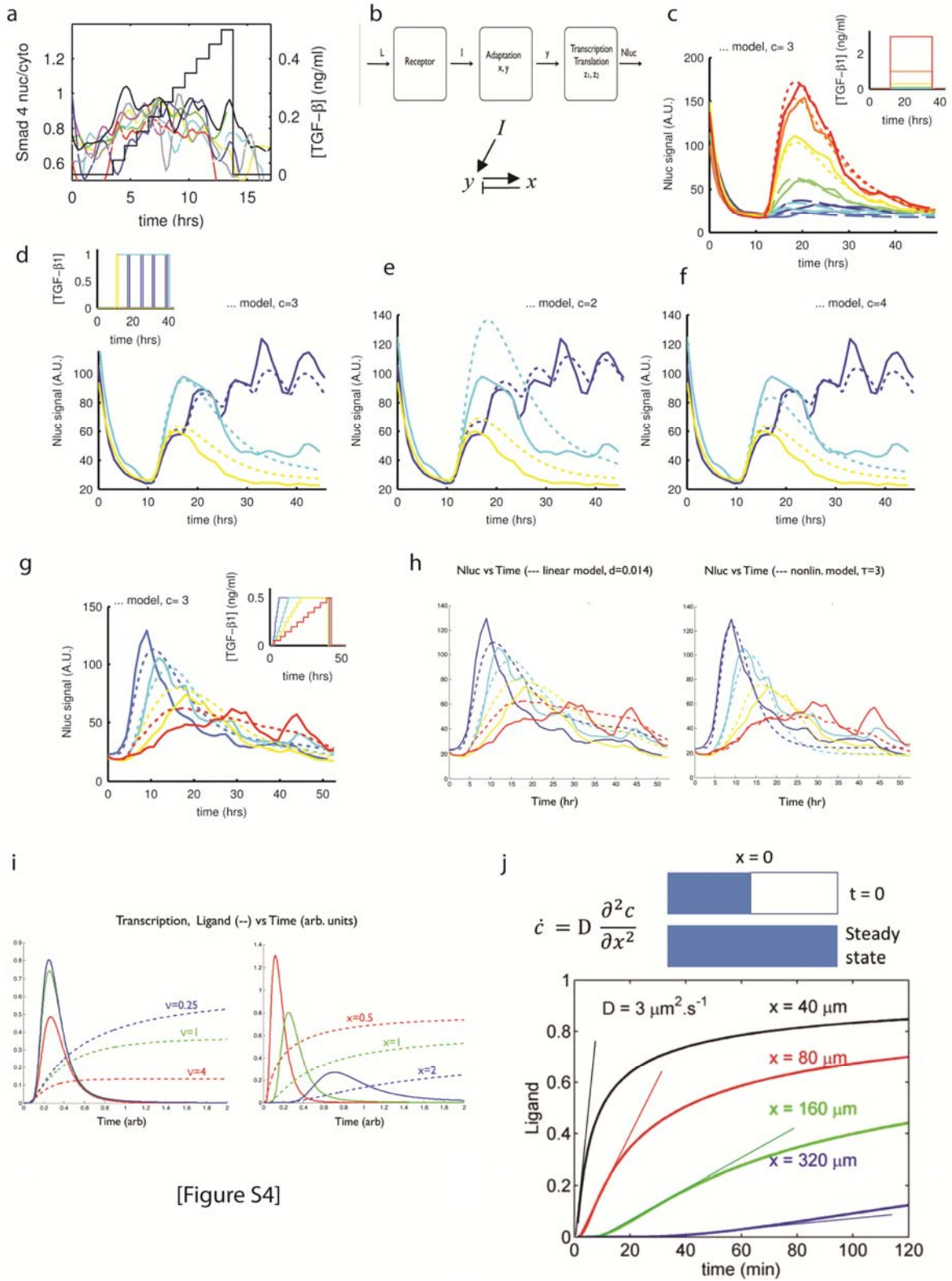


[Figure S4]

Figure S4: Additional figures for mathematical methods (related to figure 4)

a - Example of single cell traces for an experiment where the TGF- β 1 concentration is ramped from 0 to 0.5 ng/ml in 10 hours. This shows that for ramp stimulation the response is temporally incoherent, compare to steps, figure S2d-e.

b – (top) Block diagram of the computational model. L: ligand. (Bottom) arrow diagram of the adaptive block.

c- Nluc in response to a ligand step fit with the quasilinear model. The TGF- β dose in (ng/ml) vs time in steps of 3x (inset) and the Nluc transcriptional response, for corresponding colors. The meaningful fitting parameters are $c = 3\text{hr}^{-1}$, $K_i = 0.3$ ng/ml and $\tau = 5$ hr, and it is easy enough to sample a grid in three dimensions to find the global optimum. The parameter describing non-adaptation is $d = 0.006$ (see eq.5 in section 6 of supplementary methods), and its effect on these fits is negligible, but it becomes relevant for the response to ramps.

d - Nluc in response to ligand pulses. The TGF- β dose in (ng/ml) vs time (inset) and the Nluc transcriptional response, for corresponding colors. The overlay of the data for a single pulse (yellow) vs the first pulse of a series (purple) is a measure of experimental reproducibility. The fit parameters are identical to panel c but the scale factor is different.

e,f - Nluc fit varies with the adaptation parameter c in Eq.1 (section 6 of supplementary methods) . Two values c are shown to compare with the preferred value in panel (d).

g - Nluc transcription in response to ligand ramps. The TGF- β dose in (ng/ml) vs. time (left) and the Nluc transcriptional response (right), with the same fitting parameters as in the step, and pulse data panels c and d.

g,h - Fits to ramp data for various parameters. The left panel uses $d = 0.014$ to mimic failure of slow ramps to completely adapt using Eq.12 (section 6 of mathematical methods). The right panel is the best fit for Hill exponent $h = 2$ in Eq.15 and a decreased response time τ which together move the peak in the 4 hr. ramps to earlier times and the 20-40 hr. ramps to later times relative to the standard fit.

i - Transcriptional response to a diffusing, decaying ligand, (Eq. 20 section 7 of the supplementary methods). The model parameters are the same as in Fig.S4c to within an overall time scale, and for long times the ligand (dashed) varies with position as $e^{-\sqrt{k}x}$, i.e., we took $D = 1$ in Eq.20. The left panel shows the response for various values of the ligand decay rate with $x = 1$. For the smallest value of v the response saturates since the ligand varies more rapidly than the adaptation. The right panel shows the response as a function of position for $v = 0.025$, though for the time interval plotted the ligand curves are indistinguishable from the case $k = 0$.

j - Temporal profile at various distance from the source of a diffusing ligand, without degradation, Eq.17 (section 6 of supplementary methods). In that case the ligand steady state profile is flat, but the speed at which this steady state is reached depends on the distance to the source: the closer to the source, the faster the ligand concentration increases and reaches the steady state level. The straight colored lines have been added to highlight the initial slope of the temporal profiles. Hence, an adaptive pathway, sensitive to the speed of increase, can get positional information from the speed while the linear pathway cannot.

Supplementary movie 1 : sorre et al. movieS1 (related to figure 1)

This movie shows the evolution of GFP-Smad4 intracellular localization (green) in response to a step stimulation of TGF- β 1 (left panel). On the right panel the nuclear to cytoplasmic ratio of GFP-Samd4 is plotted as the movie goes (green solid line). Black solid line depicts the evolution of TGF- β 1. (mp4, 457kb)

Supplementary movie 2 : sorre et al. movieS2 (related to figure 2)

This movie shows the evolution of GFP-Smad4 intracellular localization (green) in response to a series of 3 pulses of TGF- β 1 (left panel). On the right panel the nuclear to cytoplasmic ratio of GFP-Samd4 is plotted as the movie goes (green solid line). Black solid line depicts the evolution of TGF- β 1. (mp4, 302kb)

Supplementary movie 3 : sorre et al. movieS3 (related to figure 4)

This movie shows a direct comparison of how the fates are established as a function of time downstream an adaptive and a linear signaling pathway. With the adaptive pathway, the final pattern is reached 3x faster. The Gene Regulatory Network that assigns cell fate in response to TGF- β stimulation is the one presented in Fig.4g, and discussed in details in supplementary methods section 7

(mp4, 1.6 Mb)

Supplementary methods

1 - Cell lines, Cell culture, C2C12 cell differentiation

The generation and characterization of the fluorescent cell lines we used for imaging was described previously by us²⁹. We used the ePiggyBac (ePB) transposable element system to make stable cell lines³⁰. All fusion proteins are under the control of the constitutive promoter CAG. To make the RFP-Smad2 cell line, we transfected C2C12 (ATCC) cells with ePB-B-CAG-RFP-Smad2 and ePB-P-CAG-GFP-NLS together with a plasmid encoding the ePB transposase. To make the GFP-Smad4 cell line, we first transfected ePB-B-CAG-GFPsmad4, ePB-P-CAG-Smad2, and then transfected the resulting cells with ePB-Z-CAG-RFP-H2B. The amount overexpressed Smad2 in both cell lines was checked by Western blots and was found comparable to endogenous level²⁹. The dynamic response of the transformed and parental lines was similar under all conditions tested. All C2C12 cell lines were maintained in growth medium (GM, DMEM containing 10% (vol/vol) FBS).

Differentiation experiments were performed using a sub-clone of the parental C2C12 cell line that was positive for MyoD1. Cells were seeded at $\sim 50,000$ cells/cm² in 24 wells glass bottom plates (MatTek). Differentiation protocols were started the next day, when cultures reached confluence (2 ± 1.10^5 cells/cm²). For the control, Culture medium was switched at t=0 from GM to differentiation medium (DM, DMEM containing 2% (vol/vol) Horse Serum). For the step stimulation, medium was switched at t=0 from GM to DM containing 0.1ng/ml TGF- β 1 until t=15 hours when medium was changed to DM only. For pulsed stimulations, medium was switched at t=0 from GM to DM containing 0.1ng/ml TGF- β 1, at t=1 hour the TGF- β 1 containing DM was removed from the cells and replaced by DM. The TGF- β 1 containing DM was saved and stored in the cell incubator (37C; 5%CO₂) and re-used for subsequent pulses at t=7 and 14 hours. All samples were fixed at t=24 hours. Time courses of ligand stimulation are described in Fig.2f. Comparable results were observed with 2 different MyoD1 positive clones as well as with the parental cell line. Although in the latter case the proportion of differentiating cells in the control was only about 20%, the fractional reduction under pulsed stimulation was similar to what we reported. TGF- β 1 was purchased from R&D Systems and used at the concentrations indicated in the main text.

2 - Microfluidic cell culture

Microfluidic cell culture was carried out in the cell culture chip as described in^{27,31}, see also in FigS1ab a reproduction of the chip layout. This system allows precise temporal control of ligand delivery. PDMS chips were obtained from the Stanford foundry (<http://www.stanford.edu/group/foundry/>). Feeding and imaging of the cells was computer controlled via the Matlab-based CellCultureChip software kindly provided by the Quake Lab (Stanford University) that we modified to support our hardware.

Chambers were coated with fibronectin (F1141-sigma, 20 μ g/ml, 4h incubation). About 100-200 cells per chamber were seeded (~ 10000 cells/cm²). Cells were allowed to grow for at least 12 hours before any stimulation. We checked that growth rate in the cell culture chip was comparable to the one in regular cell culture dish (see figure S2b). Growth was not negatively affected by TGF- β 1 stimulation or imaging. To that regard, we found that it was important not to use tygon (SH-L-54) for any tubing used for cell feeding or stimulation as it had a strong inhibitory effect on cell growth,

especially when new and/or autoclaved³². We used PTFE tubing (Cole Parmer, cat# EW-06417-21) instead. Cells were fed every hour by replacement of 100% of the volume of the chamber using the on-chip microfluidic pump, unless the composition of the medium was changed, in which case the medium was replaced by a 10 second flush. As regular DMEM is strongly fluorescent in the GFP channel, we used a modified version of DMEM lacking riboflavin and phenol red (custom made medium, GIBCO). This alteration had no effect on C2C12 growth or response to TGF- β 1 and greatly reduced the fluorescence background.

3 - Image analysis

Cells were imaged with a Leica DMI6000B microscope (10x 0.45NA air objective) and a Hamamatsu (OrcaR11) camera. Images were acquired every 15 min for the duration of each experiment. Image analysis was performed using custom software written in MATLAB. We used the nuclear marker images to identify nuclei using an algorithm that identifies local maxima and then detects the edges of each nucleus by examining the contour height of the maximum intensity gradient. We identified the cytoplasm of each cell either by applying a method similar to that used for the nuclear fluorescence image; when this approach was not possible (e.g., Smad2 in cells stimulated with TGF- β 1 is almost exclusively nuclear), we used a narrow donut around the nucleus with radius chosen so that it almost certainly was contained in the cell. Smad fluorescence was computed by examining the average values of nuclear and cytoplasmic fluorescence in the masks defined by this procedure.

Single cell traces were produced by a tracking algorithm adapted from²⁹. To extract the single cell response to a step or pulse stimulation single cell data were spline-smoothed (Matlab, curve fitting toolbox) prior to extrema calculation, see figure S2d for a graphical description of extraction of characteristics of single cell response.

4 – Immunofluorescence and Western blots

At the end of the C2C12 differentiation experiment (figure 2), cells were rinsed once with PBS, fixed with 4% paraformaldehyde for 20 min, rinsed twice with PBS, blocked for 30 min with 3% donkey serum and 0.1% Triton X-100 in PBS, and then were incubated overnight at 4°C with primary antibodies diluted in blocking buffer. Primary antibodies were: myogenin ([F5D], DSHB, dilution 1:400) MyoD ([5.8A], Abcam, dilution 1:400) and 12-101 (DSHB, dilution 1:200). Cells then were washed three times with PBS, 0.1% Tween 20 for 30 min each wash, incubated for 30 min with secondary antibodies (Alexa 488; dilution 1:400) and DAPI (dilution 1:10,000) diluted in blocking buffer, and washed twice more with PBS, 0.1% Triton X-100 for 30 min each wash. For the histograms of nuclear to cytoplasmic ratio of Smad3 presented in FigS2p we used and Smad3 (C67H9) Rabbit mAb from Cell Signaling Technology at a 1:100 dilution.

Cells were lysed in cell lysis buffer (Cell Signaling Technologies) containing protease and phosphatase inhibitors, and Western blotting was performed using standard techniques. The nuclear and cytoplasmic extractions presented in figure S2o were performed using the “NE-PER Nuclear and Cytoplasmic Extraction Reagents” from Thermo Scientific, following manufacturer protocol and gels were stained with Smad3 (C67H9) Rabbit mAb from Cell Signaling Technology at a 1:1000 dilution. For the western blots presented in Fig.S2n we used Phospho-Smad3 (Ser423/425) (C25A9) Rabbit mAb (1:1000), Smad3 (C67H9) Rabbit mAb from Cell Signaling Technology (1:1000) and Smad2/3 (610482; BD Transduction Labs) (1:1000)

We directly elucidate the dynamics of Smad3 activation by monitoring the intracellular localization and phosphorylation status of the endogenous Smad3 using immuno-fluorescence and western blots as a function of time. The results of these experiments are displayed in Fig.S2, panels (n,o,p) and they clearly show that Smad3 stays in the nucleus as long as TGF- β ligand is present in the culture medium, like Smad2.

To reach that conclusion, we have evaluated 2 antibodies from Cell Signaling Technology that were advertised to be specific to Smad3. Fig.S2n shows a characterization of these antibodies with western blots. To evaluate cross reactivity with Smad2, we also blotted lysates of C2C12 cells expressing a RFP-Smad2 fusion, see the 2 last columns of that gel. The p-Smad3 antibody nicely detects phosphorylation (compare column 'ctrl' and the stimulated ones) but it also at least partially detected phosphorylated RFP-Smad2. It is therefore not possible to exclude that the observed sustained response comes from Smad2. The Smad3 antibody on the other hand was specific of Smad3 as it didn't stain RFP-Smad2.

We thus went on with that antibody to measure the evolution of the intracellular localization of Smad3 using nuclear and cytoplasmic extractions, as a function of time after stimulation with TGF- β 1. Smad3, like Smad2 stayed localized in the nucleus as long as the cells are stimulated by TGF- β ligand, Fig.S2o.

Finally we used the same antibody to follow the evolution of the intracellular localization of Smad3 upon TGF- β stimulation using immunofluorescence. The conclusion is the same: Smad3, as Smad2 stayed localized in the nucleus as long as the cells are stimulated by TGF- β ligand, Fig.S2p.

5 - CAGA₁₂-Nluc: a live cell reporter for TGF- β pathway transcriptional activity

This section describes the design and validation of CAGA₁₂-Nluc as a live cell reporter for TGF- β transcription. In a previous publication²⁹ we took advantage of the homogeneous response of C2C12 cells to a ligand step to use population assays such as qRT-PCR to measure the induction of a few well-established TGF- β target genes to show that the pathway was adaptive and that the time course of transcription was consistent with the observed GFP-Smad4 dynamics.

This approach however, was inadequate for the present study, for several reasons: the length of the experiments (>48h for the ramps) made the use of qRT-PCR to construct a time course with enough temporal resolution very impractical. We want single-cell time-lapse recordings to monitor the response to the more complex temporal stimuli we apply in this paper. Finally, target genes could have their own regulation, independent of TGF- β signaling, that could cloud the interpretation of experiments lasting a day or more.

We thus turned to synthetic reporters. Several TGF- β responsive elements have been published in the literature. In our previous study, we used 2 of those (3TP, CAGA₁₂)^{28,33}, upstream of firefly luciferase and observed in an end point assay, luciferase production consistent with the adaptive response observed with the GFP-Smad4 reporter.

These TGF- β responsive elements are thus appealing candidates for a single cell TGF- β reporter system. Our initial attempts used the CAGA₁₂ responsive element to drive expression of either GFP or Firefly luciferase. Unfortunately, these reporters didn't produce enough signal for detection at the single cell level.

We thus switched to NanoLuc luciferase (Nluc), a small (19.1kDa) engineered luciferase commercially available from Promega³⁴. The enzyme is advertised to be 150 fold brighter than other luciferases. It uses furimazine, a coelenterazine analog, as a substrate to produce a glow-type luminescence signal with a half-life of about 2 hours in lytic assays.

We designed 2 clonal C2C12 cell lines with Nluc reporters stably integrated in the genome using the ePiggyBAC transposable elements system. In the first line, used to perform controls and validation experiments, Nluc production is under the control of the constitutively active promoter CAG. In the second cell line, used for the signaling experiments, Nluc expression was driven by the TGF- β responsive element CAGA₁₂. To improve visibility and facilitate automated image analysis, Nluc was fused with a nuclear localization signal (NLS) and deployed in cells that also expressed the fluorescent nuclear marker RFP-H2B. See vectors, FigS1c-e.

When constitutively expressed (from the CAG promoter), Nluc luminescence could readily be detected in single cells with exposure times on the order of a few seconds (objective: 10x 0.45 NA; camera: Hamamatsu ORCA R2, maximum gain, binning 4), Fig.S1f. For the CAGA₁₂ responsive element, luminescence signal could be detected in single cells with a 2 minute exposure time. Importantly, a several-fold increase of the signal could be observed 6 hours after initiation of TGF- β stimulation, Fig.S1gh

Motivated by this encouraging preliminary result, we next tried a time course of nano-luciferase expression. In regular cell culture conditions (DMEM+10% FBS; 37C; 5%CO₂; MatTeK glass bottom 35mm dish) we observed a very short-lived luciferase signal (half-life <1h), even when the luciferase expression was driven by the constitutive promoter CAG, Fig.S1i. This result is consistent with the fact that the half-life of the luminescence signal in lytic assays is on the order of 2 hours, and that this half-life is expected to be further reduced at cell culture temperature and in the presence of serum (manufacturer instructions). The fact that the signal intensity was restored by providing fresh substrate (Fig.S1i) further confirmed that the Nluc substrate was not stable in these conditions and therefore not suitable *as is* to monitor TGF- β transcriptional activity over a long period of time in an unattended fashion.

Similar issues have already been reported for Renilla luciferase substrate coelenterazine-h. In that case, measuring luminescence in living cells over long times was made possible by modifying the substrate chemical structure in order to prevent its spontaneous auto-oxidation³⁵. An analogous protected substrate for Nluc is not yet available, but as it also produces light by catalyzing its substrate oxidation, we hypothesized that the observed loss of substrate stability was due to spontaneous auto-oxidation. We exploited the capabilities of the Cell Culture Chip, to design the following protocol for long-term live cell luminescence imaging:

- Over the course of the experiment, the substrate (diluted 1:500 in DMEM w/o phenol red, [furimazine] = 10 μ M) is kept in a refrigerated vial, in an O₂ free atmosphere (pressurized with 95%N₂; 5%CO₂). This vial is connected to one of the CCC inputs via a capillary (I.D. 75 μ m) to minimize dead volume, Fig.S1j.
- Just before measuring cell luminescence, fresh substrate is flowed over the cells for 10 seconds and the image acquired. Following image acquisition, the media is replaced by

regular medium (+/- TGF- β). This has the extra advantage of minimizing cell exposition to substrate, thus reducing its potential toxicity.

Figure S1k shows a time course of luminescence of Nluc-NLS, under the control of the constitutive promoter CAG, acquired using the above described protocol once every 2 hours. The signal still decays, but much slower than in the dish experiments discussed earlier (Fig.S1i), and it stabilizes at about 50% of its original value. Providing freshly diluted substrate doesn't increase the signal in these conditions, suggesting that the observed decay is not due to substrate degradation anymore but rather to an "activity-induced" inactivation of the enzyme. Indeed, when the frequency of luminescence measurement is reduced from 1 picture every 2 hours to 1 picture every 6 hours, signal decay is no longer observed.

The lower average luminescence value reached at steady state thus reflects the apparent reduction in Nluc lifetime when imaged at a given frequency. The Nluc half-life was thus measured as ~5hrs when luminescence was acquired every hour, a 2-fold reduction compared to the un-imaged situation, measured in by treating cells with the protein synthesis inhibitor cyclohexamide (not shown).

In all the experiments presented in the main text of this paper, luminescence was measured every hour and we waited for the luminescence signal to reach its steady state (typically 15 hours) before stimulation with TGF- β . Figure S1l shows the full time course for Fig.1k in the main text.

6 Mathematical Model for Fitting Nluc time courses

6.1 Introduction

In order to unify all the dynamic data we obtained for Nluc in response to steps, pulses and ramps we have fitted them all to a single model. This establishes consistency among the experiments and also consistency with the Smad4 data for adaptation. Microfluidic technology if used with suitably engineered cells, allows the application of stimuli matched to the cellular dynamics of interest. The stimuli can then elicit substantial changes in output eventhough the read out, in our case transcription, is much slower than aspects of the signaling system one wants to explore. Thus a quantitative model, such as we provide here, is then needed to infer the internal process e.g., adaptation, from the Nluc readout.

Prior models for the TGF- β pathway have focused on nuclear-cytoplasmic shuttling or receptor adaptation via the inhibitory Smads [Schmierer et al., 2008, Vilar et al., 2006]. While all these processes are part of the signaling pathway, they omit the predominant feature of our dynamic measurements which is the rapid adaption by Smad4, while Smad2 and by inference the receptors remain active. Secondly numerical parameters depend on cell type, growth media, etc so we are forced to rely solely on our measurements to fit a model. This dictates a model that decomposes signal transduction into three blocks and parameterizes each by an input-output relation Fig. S4b; nothing more detailed can be fit. It has been shown quite generally that multi-parameter models fit to typical biological data leave many directions in parameter space completely unconstrained [Gutenkunst et al., 2007]. Such fits are illusions since they generally are not predictive in situations outside of the realm they were fit in.

We wish to quantify the degree of internal consistency among our various dynamic stimuli. We thus fit to a model with only three essential parameters (after allowing for a scale factor to define microscope camera units) each of which can be tied fairly tightly to a single experiment. This model is quasi-linear since fully nonlinear models used more parameters, and required fine tuning to make marginal improvements to the quality of the fits. We also limit ourselves to modeling the population response of the Nluc expression data. This is because it is obtained only every hour for technical reasons which is the response time of the single cell Smad4 data, Fig S2d. Attempting to model the cell-cell fluctuations would entail more parameters, and when these are multiplicative, averaging over the parameter ensemble can not be interchanged with time integration. Thus a nominally cruder model for the population averaged data may be more informative.

The most crucial module in Fig. S5b is the adaptive one, so we consider that first and then add the other steps.

6.2 Minimal Model for Adaptation

A linear model for adaptation has the fewest free parameters and will prove adequate for our data. Its functional form is unique if we insist that the variable y adapts to a fixed point of 0. We use I as the ligand dependent input.

$$\dot{x} = y \tag{1}$$

$$\dot{y} = -bx - cy + I \tag{2}$$

We assume $b > 0$ since we want a positive value of x at the fixed point, and $c > 0$ for stability. The two free constants define the two eigenvalues of the 2x2 matrix which are the only degrees of freedom available after rescalings. If we insist on real eigenvalues then $c^2 \geq 4b$. The fastest adaptive response for a given rise time is obtained when the two eigenvalues are degenerate. We use this limit henceforth, since it eliminates a parameter and is in tolerably good agreement with the single cell Smad4 data. Thus following an input step at $t = 0$ we have ($c^2 = 4b$)

$$y = Ite^{-ct/2} \quad (3)$$

Equations (1)-(2) can be solved when I varies linearly from 0 to I_0 over the time interval $[0, T]$ by simply taking a time derivative of the \dot{y} equation and shifting \dot{y} to remove \dot{I} :

$$y = \frac{4I_0}{Tc^2}(1 - (1 + ct/2)e^{-ct/2}) : 0 < t < T \quad (4)$$

When $cT \ll 1$, $y(T) \simeq I_0T$, which agrees with the change in $y(t)$ computed for a step change in I from Eq. (2) for $ct \ll 1$. It is also useful to break the perfect adaption as in Eq.5 so as to fit experiments, that show the 'plateau' discussed in Suppl IV,. The fixed point is then displaced from $y = 0$ by an amount $\sim dI$.

$$\dot{x} = y - dx \quad (5)$$

For reference in subsequent discussions several conventional adaptive models should be listed:

$$\dot{x} = I - bx \quad (6)$$

$$\dot{y} = I - xy \quad (7)$$

$$\dot{x} = 1 - Ix \quad (8)$$

$$\dot{y} = Ix - by \quad (9)$$

$$\dot{x} = I - ax \quad (10)$$

$$\dot{y} = I(1 - y) - bxy \quad (11)$$

In Eqs. 6-7 the input creates both the adaptive variable and an inhibitor x that causes the degradation of y , while Eq.8-9 could represent a protein-protein interaction between the input and x to create a complex, y , that adapts. Equations 10-11 describes a 'push-pull' system where I catalyses the conversion of y to an active form, and x with some delay converts it back. Each term in Eq.11 can be generalized to Michaelis-Menton form. We have minimized the number of constants in all equations by rescaling x, y, I and the time. The two nonlinear equations would have more parameters than the linear system if all terms of comparable order were included.

To begin eliminating models, note that Eq.1-2 depends only on the difference in I levels for a step while Eqs.6-9 depend approximately on the ratio of I levels before and after the step, and Eqs.10-11 are more complex. Also the adaptation time varies with the inverse input level in some regimes, i.e., I has units of frequency.

While it is cumbersome to solve Eqs.6-11 for a ramp input, useful intuition for what follows can be obtained in the regime where the ramp duration T is much larger than any other time in the problem. Then it is easy to show by appropriately rescaling the dependent variables x, y with I that y is displaced from its fixed point value by $O(\frac{1}{T})$ for the duration of the ramp. This also agrees with the solution of the linear model, Eq. 4 when $cT \gg 1$.

With these mathematical facts we can confront the data. We prefer the linear model since it naturally gives rise and fall times for the response that are ligand independent, and the temporal profile is a good fit to the Smad4 data for single cells Fig S2d-j. It is hard to eliminate I from the time scale in the nonlinear models and still get a large response (for small fractional changes in I all models are effectively

linear). All models undershoot in y following a downward step, and thus disagree with the Smad4 data. Furthermore while y in the linear model is always positive for non decreasing $I(t)$, it becomes negative when I jumps down and thus can not represent a concentration. So in all cases there must be a nonlinear transformation between y and Smad4 that flattens out y values that fall below the fixed point, while preserving the excursions above the fixed point. So a relation like $\text{Smad4} \sim \ln(1 + a_1 e^{a_2 y})$ would work for the linear model or more generally $y^m / (K_*^m + y^m)$. Since we do not have any detailed data for decreasing stimulation levels we prefer the quasilinear approximation that $\text{Smad4} \sim \max(0, y)$

The ideal way to distinguish the linear from the nonlinear models would be examine the response to ligand steps with various levels both before and after the step. The linear model would depend on the difference in levels while the nonlinear ones would register the ratio, i.e., they follow Weber's Law. Molecular noise and cell-cell variability make it difficult to achieve the necessary range in I , and also saturation could happen upstream of the adaptive variables, thus I will vary by less than the ligand itself. The data for E.coli chemotaxis allows a convincing fit to a more elaborate though still phenomenological adaptation model [Tu et al., 2008]

6.3 Quasilinear model for transcription.

The dependence of both Smad4 and Nluc in response to a ligand step L scales as $L/(K + L)$, Fig.1, so it is plausible to simply model the receptor module in Fig. S4b and its connection to adaptation by

$$I = L/(K_I + L) \quad (12)$$

For the transcriptional output we propose

$$\dot{z}_1 = \max(0, y) - z_1/\tau \quad (13)$$

$$\dot{z}_2 = z_1 - z_2/\tau \quad (14)$$

where z_1 can loosely be thought of as message, and z_2 as protein. The relaxation time τ need not be the same in the two equations, but since the data requires $\tau \sim 5$ hrs, while the adaptive system has a time scale of ~ 1 hr, the time course of z_2 is largely insensitive to how relaxation time is distributed between the two equations, so we made the rates equal, thereby eliminating a parameter that would be impossible to fit.

6.4 Fits to time course data

We are now in a position to consider the compatibility among the step, pulse and ramp data in Figs 1,2,3. All conditions for each type of data were run at the same time with uniform cell densities, but we do not have complete control over the cell seeding, or the batches of ligand or Nluc substrate. Thus we use a different scaling factor for each data set. As an internal standard we include a ligand step to a level above K_I in the pulse and ramp data sets. The model takes the ligand time course used in the experiments. For plotting, the Nluc level just prior to simulation is added to the scaled model output.

The response to variable height steps is well fit as regards to its rise, fall and max, Fig.S4c. The transcriptional response to pulses will determine $c \sim 3$, which means that y peaks at a time of 0.67 after stimulation. Thus to delay the peak of z_2 to around 6 hrs, we added another step in the cascade which means that z_2 begins as $t^3 e^{-ct/2}$. The peak position is also influenced by τ , but the decay rate following the step is more sensitive to τ , and the fit is clearly reasonable. Note there is no suggestion that time scales depend on the magnitude of the step.

In Fig.S4d we show the response, to a single pulse, repeated pulses with a 6 hr period ($\sim \tau$) and a step for calibration. The relative amplitude of a single pulse and a step is sensitive to c in Eq.3, since as

the exposure time to ligand tends to zero, so must the transcriptional output, and c supplies the units for time. The accumulated response to periodic pulses is a balance of the decay described by τ and production. So it is a test of the model that the same τ works for both pulse and step data. Figure S4ef show how the fit degrades for $c = 2, 4$ in comparison with the preferred value of 3. The value of c corresponds to a characteristic time of 0.67 which is in good agreement with the histogram of single cell Smad4 responses in Fig.1h, given the uncertainties in averaging over the population. Note any correlation in between the time of the peak and the size of the Nluc response will be reflected in the population average. Thus the agreement is confirmation that microfluidics can be used to tailor dynamic stimuli commensurate with rapid events internal to the signaling pathway, whose consequences can then be read out through the much slower transcriptional time scales.

The ramp data is the most challenging to fit with our linear model, Fig.S4g, particularly the slowest one that lasts 40 hrs. However experiments running this long under TGF β stimulation are susceptible to the multiple small systematic effects that we discuss in Suppl IV, plateaus. We can partially account for these effects with the parameter allowing incomplete adaptation, Fig.S4h left. The best fit to the ramp data is obtained by replacing Eq.12 with a similar expression with Hill exponent 2 and shortening τ to 3 from 5, Fig.S4h right

$$I = L^2/(K_I^2 + L^2) \quad (15)$$

A Hill exponent of 2 does not fit the step data, and would under predict the lower ligand levels. (The preferred τ of 3 is within the accuracy of the experiments since $\tau = 4$ would give almost indistinguishable fits for the step and pulse data, and we do not consider a 20% parameter change material). The reason a Hill exponent improves the fit is seen by computing the time derivative of I which by our treatment of adaptive models is the amount y is displaced from 0 by the ramp. Since $\dot{I} = \frac{hL^{h-1}\dot{L}}{(K_I^h + L^h)^2}$, for an exponent, $h > 1$, \dot{I} increases with L when L is small. This pushes the time of peak response later for the slower ramps as observed.

We have been unable to obtain better fits to the ramp data using the other adaptive models together with Eq.12 for essential the same reason as for Eq.1-2, i.e. \dot{I} decreases with L . Another possibility to improve the ramp data fits, while preserving the scaling of the step data with $L/(K_I + L)$, is to replace Eq.13 with

$$\dot{z} = y^{(n+1)}/(y^n + (\frac{K_z}{I})^n) \quad (16)$$

If the maximum of y for the smallest steps was greater than y in the slower ramps (only marginally true), then K_z could be chosen such as to preserve Eq.13 for the steps but would add additional factors of L for the ramps. One could rationalize the I dependence in Eq.16 as arising from Smad2, that has to dimerize with Smad4 to make a transcriptionally active complex. The ratio of terms in Eq.16 could arise from the combination of cooperative activation and repression.

7 A Model for Dynamic Embryonic Patterning

7.1 An adaptive pathway can extract positional information without a steady state gradient

To reinforce the intuition conveyed in Fig.4 of the main text that adaptive systems can infer position from the rate the ligand changes in time, we reconsider several steps in that argument in a more mathematical fashion, focusing on limits where analytic results can be obtained. Consider the case of one dimensional diffusion with no degradation, so the final static concentration profile is flat and thus confers no positional information. If we turn on ligand at $t = 0$ and fix its value at $x = 0$ to $L = 1$ for all subsequent times then its value for $t, x > 0$ is

$$L(x, t) = \operatorname{erfc}(x/(2\sqrt{Dt})) \equiv \frac{2}{\sqrt{\pi}} \int_{x/(2\sqrt{Dt})}^{\infty} e^{-y^2} dy \quad (17)$$

where D is the diffusion constant. To represent the diffusion around a circle of circumference $2W$ with the ligand fixed at $x = 0$, or diffusion in a box of length W one would use $L = \operatorname{erfc}(x/(2\sqrt{Dt})) + \operatorname{erfc}((2W - x)/(2\sqrt{Dt}))$. An idealized but still informative model for the transcriptional output from an adaptive system is just $\int_0^t (\dot{L})^2$. If the power of \dot{L} was one, the formula just reduces to the usual morphogen model with output $\sim L(t)$. A power larger than one, penalizes slow rates of change. Computing \dot{L} from 17, we find:

$$\int_0^t (\dot{L})^2 = (1 + x^2/(2Dt))e^{-x^2/(2Dt)}/(\pi x^2) \quad (18)$$

For long times $t \gg x^2/D$ the result scales as $1/x^2$ which could have been deduced by dimensional analysis since the net dimension of $\int_0^t (\dot{L})^2$ is inverse time. Our 'toy' model encapsulates the tendency of adaptive systems to suppress low frequencies. However this model lacks an intrinsic time scale for the network implementing the adaption, thus the response diverges as $x \rightarrow 0$, while it should saturate for a ligand step.

A more realistic model for ligand spreading in an embryo would include ligand degradation at a rate k , as in the following:

$$\partial_t L(x, t) = D\partial_x^2 L(x, t) - kL(x, t) \quad (19)$$

$$L(x, t) = \frac{x}{2\sqrt{\pi D}} \int_0^t s^{-\frac{3}{2}} e^{-ks - \frac{x^2}{4Ds}} ds \quad (20)$$

Equation 20 was derived from the Laplace transform of Eq.19. For $k = 0$, its' time derivative is identical to that of Eq.17. For $t = \infty$, Eq.20 becomes $L(x) = e^{-\sqrt{k/D}x}$. This fact may be verified by taking the x-derivative of Eq.20, doing a strategic integral by parts in s and then another derivative in x . One then obtains $\partial_x^2 L(x) = \frac{k}{D}L(x)$ which proves the point.

7.2 Consequences for fate decision

In Fig.4g-i we use our quasilinear adaption model Eqs.1,2,12,13,14, together with Eq.20, to make the point that the transcriptional output from adaptive system can reach its maximal value and thus infer position well before the ligand reaches its asymptotic value. However the output from any adaptive system returns to zero, thus we have to assume a bistable gene regulatory network (GRN) in place of Eqs.13,14 to capture the output and render it permanent. This is very consistent with standard embryology. A

signal is applied during a window of competency, at the end of which the fate of the targets is specified and no longer requires the signal.

A minimal model requires two proteins, A, B both bistable. They define three territories in order of decreasing signal level: A ON B OFF; A OFF B ON; both OFF. The equations are:

$$\dot{A} = m(t) + \frac{A^2}{1 + A^2} - \nu_A A \quad (21)$$

$$\dot{B} = (m(t) + \frac{B^2}{1 + B^2}) \frac{1}{1 + A^2/K_A^2} - \nu_B B \quad (22)$$

where $m(t)$ is a time dependent (morphogen) input to the GRN to be defined subsequently. Without loss of generality, we can always rescale A, B to make the constant in the $1/(1 + X^2)$ terms one. We also assume that the response time of the GRN is fast compared to the natural time scale of the morphogen and the adaptive module, which can always be accomplished by multiplying the time derivative terms on the left by a constant. The initial conditions are $A = B = 0$. We then chose constants such that A requires the highest morphogen levels to switch from OFF to ON and when ON represses B , which is more sensitive to morphogen. The B domain is defined by where A is OFF and the morphogen level is high enough to switch B ON.

When $m = 0$, Eq.21 has to be bistable, which requires $\nu_A < \frac{1}{2}$. To simplify the algebra we in fact assume $\nu_{A,B} \ll 1$. Then A ON corresponds to $A = \frac{1}{\nu_A}$. The A OFF state disappears by a saddle-node bifurcation when $m > m_A = \frac{\nu_A^2}{4}$. The OFF state for any $m < m_A$ satisfies $A < \nu_A/2$ and thus if we chose $K_A \sim \nu_A$ the inhibitory factor in the B equation is larger than $\frac{4}{5}$. Thus the saddle node bifurcation when the B OFF state disappears and the system jumps to the ON state occurs for $m_B \sim (\frac{5\nu_B}{4})^2/4$ following the same algebra as for A . For A ON, the inhibitory factor in Eq.22 becomes $\sim \nu_A^4$ and easily blocks all response. To order the A, B expression domains appropriately we chose the decay rates ν to make $m_B < m_A$.

In the last figure of the main text we compared the output of the adaptive system ($I = L(x, t)$) Eqs.1,2 with the so called linear one, $\dot{y} = L(x, t) - cy$ when subject to the time and space dependent ligand in Eq.20. Since we need place the A, B expression domains in the same place we relate $m(t)$ in Eqs.21,22 to y with by $m = c_1y + c_2y^2$ where the constants $c_{1,2}$ are chosen separately for the two models for y .

Supplementary references

- 27 Gómez-Sjöberg, R., Leyrat, A. A., Pirone, D. M., Chen, C. S. & Quake, S. R. Versatile, fully automated, microfluidic cell culture system. *Anal Chem* **79**, 8557-8563 (2007).
- 28 Dennler, S. *et al.* Direct binding of Smad3 and Smad4 to critical TGF beta-inducible elements in the promoter of human plasminogen activator inhibitor-type 1 gene. *EMBO J* **17**, 3091-3100 (1998).
- 29 Warmflash, A. *et al.* Dynamics of TGF- β signaling reveal adaptive and pulsatile behaviors reflected in the nuclear localization of transcription factor Smad4. *Proc Natl Acad Sci USA* **109**, E1947-1956 (2012).
- 30 Lacoste, A., Berenshteyn, F. & Brivanlou, A. H. An Efficient and Reversible Transposable System for Gene Delivery and Lineage-Specific Differentiation in Human Embryonic Stem Cells. *Cell Stem Cell* **5**, 332-342, doi:10.1016/j.stem.2009.07.011 (2009).
- 31 Tay, S. *et al.* Single-cell NF-kappaB dynamics reveal digital activation and analogue information processing. *Nature* **466**, 267-271 (2010).
- 32 Price, N. M., Harrison, P. J., Landry, M. R., Azam, F., Hall, K. J. F. Toxic effects of latex and Tygon tubing on marine phytoplankton, zooplankton and bacteria. *Mar. Ecol. Prog. Ser.* **34**, 41-49 (1986).
- 33 Wrana, J. L. *et al.* TGF β signals through a heteromeric protein kinase receptor complex. *Cell* **71**, 1003-1014, doi:[http://dx.doi.org/10.1016/0092-8674\(92\)90395-S](http://dx.doi.org/10.1016/0092-8674(92)90395-S) (1992).
- 34 Hall, M. P. *et al.* Engineered Luciferase Reporter from a Deep Sea Shrimp Utilizing a Novel Imidazopyrazinone Substrate. *ACS Chemical Biology* **7**, 1848-1857, doi:10.1021/cb3002478 (2012).
- 35 Hawkins, E. *et al.* Measuring Renilla Luciferase Luminescence in Living Cells. *Bioluminescence & Chemiluminescence. Progress & Current Applications* **149** (2002).
- 36 Schmierer, B., Tournier, A. L., Bates, P. A. & Hill, C. S. in *Proc Natl Acad Sci USA* Vol. 105 6608-6613 (2008).
- 37 Vilar, J. M. G., Jansen, R. & Sander, C. Signal Processing in the TGF- β Superfamily Ligand-Receptor Network. *PLoS Comput Biol* **2**, e3, doi:10.1371/journal.pcbi.0020003 (2006).
- 38 Gutenkunst, R. N. *et al.* in *PLoS Comput Biol* Vol. 3 1871-1878 (2007).
- 39 Tu, Y., Shimizu, T. S. & Berg, H. C. Modeling the chemotactic response of Escherichia coli to time-varying stimuli. *Proc Natl Acad Sci USA* **105**, 14855-14860 (2008).